A THESIS FOR THE DEGREE OF MASTER SCIENCE

Effect of transition metals on hydrothermal liquefaction (HTL) of agricultural residues

전이 금속을 적용한 농업 부산물의 수열반응에 관한 연구

By Jae Hoon Lee

PROGRAM IN ENVIRONMENTAL MATERIAL SCIENCE
GRADUATE SCHOOL
SEOUL NATIONAL UNIVERSITY
February, 2016

Abstract

Effect of transition metals on hydrothermal liquefaction (HTL) of agricultural residues

Jae Hoon Lee
Program in Environmental Material Science
Graduate School
Seoul National University

Hydrothermal liquefaction (HTL) of two agricultural residues, empty fruit bunch (EFB) and coconut shell (CCNS) was performed with an autoclave reactor within a diverse temperature range (240–330 ℃) in the presence of various transition metal chlorides ($ZnCl_2$, $CuCl_2$ and $NiCl_2$) to investigate its effects on the properties of HTL products: HTL oil, hydrochar, and water soluble fraction (WSF). The highest yield of HTL oil from EFB was 24.2 wt% at 300 ℃, which was higher than that from CCNS (14.0 wt%) at the same temperature. The yield of gas showed an inversely proportional correlation to the yield of HTL oil. At 240 ℃ the yield of hydrochar from EFB was higher than 50% due to the incomplete degradation of cellulose, and it steadily decreased with increases in temperature. Water content of HTL oil ranged from 2.0% to 5.6% for EFB, 3.3% to 9.6% for CCNS, respectively. Total acid number (TAN) value of oil for both biomasses increased with a rising temperature up to 300 ℃ and then decreased at 330 ℃. Gas chromatography-mass spectrometry (GC/MS) analysis revealed that HTL oils from EFB and CCNS at 300 ℃ had the largest amounts of chemical compounds, such as furfural and cyclic ketones derived from holocellulose and phenol, guaiacol, and syringol derived from lignin. In the presence of transition metals, the yield of HTL oil decreased with an increased transition

metal dose of up to 10.0%, while changes in the amount of gas, WSF, and hydrochar were different by according to the kind of feedstock or metals. Water content of HTL oil rose by the increasing amount of the metals, while the TAN value was varied and chemical compounds decreased. γ-Valerolactone (GVL) and levulinic acid were found, derived from acidic hydrothermal decomposition of cellulose. Unlike other metals, relatively small amounts of GVL and large amounts of levulinic acid were detected, especially in the presence of CuCl2. It is suggested that CuCl2 inactivates the conversion of levulinic acid to GVL under subcritical condition.

Key words: biomass, thermochemical conversion, hydrothermal liquefaction, transition metal, HTL oil

Student number: 2014-20040

Contents

List of Tables

List of Figures

1. Introduction

1.1. Agricultural residue and its application

Lignocellulosic biomass is classified into woody biomass and non-wood materials, which are known as non-woody biomass. There is no clear-cut division between woody and non-woody biomass, but generally, non-woody biomass includes agricultural crops for obtaining sugar and oil, herbaceous plants, and processing residues (Hakeem et al., 2014). As a primary source of non-woody biomass, agricultural residues are abundant and inexpensive. Traditionally agricultural residues are used as organic fertilizer, animal fodder, and bedding, or are simply discarded. Due to their poor utilization, value-added use of agricultural residues is critically important. Typical examples of agricultural residues include empty fruit bunch (EFB) and coconut shell (CCNS).

EFB is a residue from the palm oil industry; the industry occupies around 40% of the global vegetable oil market. Approximately one fourth of all palm biomass from the palm industry is EFB (Geng, 2013). In Indonesia, 13.8 million tons of dried EFB are produced per year (Ahn et al., 2014). In the past, EFB was usually incinerated and its ash was used as a fertilizer or soil conditioner. However, due to the smoke emitted resulting in pollution, the Department of Energy limited EFB incineration (Yusoff, 2006). Nowadays, EFB is used for mulching or soil nourishing (Kerdsuwan & Laohalidanond, 2011). However, much

larger amount of EFB is produced, causing a serious environmental problem. While not the same as EFB, problems caused by CCNS and associated coconut plantations, are also serious. For this reason, new applications of EFB and CCNS are essential.

Many investigations are in progress to add high value to agricultural residues, for example, fiber-cement (Soroushian et al., 2004), fiber-plastic composite (Nyambo et al., 2010), and adsorbent (Nasernejad et al., 2005). Also, conversion of agricultural residues to energy resources is a promising technique. The problem of rapid climate change requires a reduction of fossil fuel use to cope with climate change, agricultural residue, especially EFB and CCNS, can provide some of the cheapest renewable resources as alternatives to fossil fuels.

The two most common conversion processes are biochemical and thermochemical conversion. Biochemical conversion involves breaking down biomass to produce sugars that can be converted to bio-ethanol and other chemicals with enzymes, microbes, and catalysts. Thermochemical conversion process involves the degradation and repolymerization of biomass using heat and catalysts. Research in thermochemical conversion focuses on the production of liquid/gaseous fuels and upgrading their physicochemical properties.

1.2. Thermochemical conversion process

Biomass can be converted into a source of direct heat and power or liquid/gaseous fuels by thermochemical conversion. The processes for thermochemical conversion can be split into several groups: combustion, pyrolysis, gasification, and liquefaction.

Combustion of biomass is the process of obtaining direct heat and power by burning raw or pelletized biomass under normal air conditions. During the combustion process, chemical energy in biomass is released and hot gases (over 800 ℃) are produced and used for heat and power generation. While it is old-fashioned, it is still the dominant process for converting biomass to energy.

Pyrolysis is the thermal degradation of dried biomass occurring in the absence of oxygen. A liquid product that is dark brown and proximate to biomass in elemental composition (bio-oil), char (biochar), and gases are produced from this process (Bridgwater, 2012). Lower reaction temperatures and longer residence times increase the production of char (slow pyrolysis), and higher reaction temperatures and shorter residence times increase the production of gas and liquid product (fast pyrolysis) (Bridgwater, 2012).

Gasification involves the thermal decomposition of biomass to intermediate gases (CO, CO_2) called syngas that can be converted to liquid fuels at a high temperature (above 800 ℃). Tar and char also react with steam or hydrogen in the reactor, producing additional products. Gases are converted to heat, power, and various alcohol

products, such as methanol, ethanol, n-propanol, n-butanol, and n-pentanol. The composition and quality of gas depends on temperature, pressure, feedstock, reactor type, catalysts, gas cleanup, and conditioning (Demirbas, 2007).

Liquefaction of biomass, sometimes called the biomass to liquid (BTL) process, is a thermochemical conversion where liquid is obtained from wet biomass. Different liquid compounds are produced within the range of 300–350 ℃ and 5–20 MPa, for about 30 min of reaction time. The liquefaction process often uses catalysts in the presence of hydrogen. However, there is also non-catalytic liquefaction, often called direct liquefaction. There are some differences between liquefaction and pyrolysis. Liquefaction occurs at lower temperatures and higher pressures than pyrolysis. There is no need to dry feedstock for liquefaction, in contrast to pyrolysis that requires a drying process. Various liquids are used as solvents, for example, methanol, ethanol, acetone, etc. Among them, liquefaction in the presence of water is called hydrothermal liquefaction (HTL) (Toor et al., 2011).

1.3. Hydrothermal liquefaction (HTL) for oil production

HTL is generally carried out between 280 and 370 ℃ and 10–25 MPa. During the process, high pressure is applied to keep water in a liquid state, preventing it from becoming gaseous. This phase, known as subcritical water, has a range of unique properties. When the water is heated, its dielectric constant and the strength of hydrogen bonds between molecules decreases and the concentrations of H_3O+ and OH- ion increase (Brunner, 2014). Above 200 ℃, water is a much better solvent for hydrophobic organics and acts as an acid/base catalyst (Brunner, 2014). Organic compounds in lignocellulosic biomass such as cellulose, hemicellulose, and lignin are, therefore, dissolved in subcritical water. Main products from HTL of biomass are crude-like liquid (HTL oil), char (hydrochar), water–soluble fraction (WSF) and gas. HTL oil is much different from fast pyrolysis oil, with the former being more hydrophobic and viscous, but less dense than the latter (Elliott et al., 2015).

All of the biomasses can be considered as feedstock for HTL, from algal biomass to agricultural residues (Duan & Savage, 2011; Ross et al., 2010; Harry et al., 2014; Singh et al., 2015; Karagöz et al., 2005; Christensen et al., 2014). A wide variety of catalysts for the HTL process have been studied: alkali salts (Akhtar et al., 2010; Kumar & Gupta, 2009; Zhu et al., 2015; Liu et al., 2006), noble metals (Duan & Savage, 2011), acids (Harry et al., 2014; Zhang et al., 2009), and zeolites (Harry et al., 2014). There is a consensus that alkali salts, such

as Na_2CO_3 or K_2CO_3, are efficient catalysts for increasing HTL oil yield.

Because of the harsh process conditions, especially high pressure, the industrialization of the HTL process is still undergoing various trials. Most work on HTL has been carried out at the lab scale, but a few pilot programs are ongoing in facilities such as the Lawrence Berkeley Laboratory, Albany Biomass Liquefaction Experimental Facility, Hydrothermal Upgrading (HTU) plant, Catalytic Liquefaction (CatLiq) and Thermo-Depolymerization (TDP) process (Elliott et al., 2015; Toor et al., 2011).

1.4. Objectives

HTL of biomass is one of the most promising techniques for liquid fuel production. Liquid fuel has the potential to contribute to the global needs for transport fuels and chemical feedstock. However, most of the studies of HTL have focused on algal and woody biomass as feedstock, not on non-woody biomass. In addition, few studies have investigated non-alkali catalysts or conditions, especially transition metals. Therefore, its effect and physicochemical properties of products are not perfectly understood.

For these reasons, this study focuses on the liquefaction of agricultural residues with various transition metal catalysts and characterization of HTL products. Two different agricultural residues, EFB and CCNS, were used as feedstock in this experiment. Three transition metal chlorides ($CuCl_2$, $NiCl_2$, $ZnCl_2$) were used to investigate their catalytic effect. All experiments were performed in an autoclave reactor composed of a heater, reactor, stirrer, and cooling system.

At first, non-transition metal HTL processes of EFB and CCNS were carried out under a range of temperatures to establish optimal temperature conditions for maximizing HTL oil yield.

Second, HTL processes in the presence of transition metals were carried out with the three different metals at the optimal temperature conditions established in the previous step.

Third, the difference in mass balance of their products and

physicochemical properties of HTL oil was analyzed by various analytical methods.

Finally, the results were compared with those from EFB and CCNS to determine the effect of transition metals on the HTL process and its major products.

2. Literature review

2.1. HTL of biomass

2.1.1. Feedstock for HTL

2.1.1.1. Cellulose / lignin model compounds

Liquefaction of the main constituents of lignocellulosic biomass (cellulose, hemicellulose, and lignin) was carried out to prove the basic reaction pathway for liquefaction of whole biomass. Sasaki et al. (Sasaki et al., 2000) performed the decomposition experiment of microcrystalline cellulose in subcritical and supercritical water. They found that hydrolysis products were mainly obtained at 400 ℃, while aqueous decomposition products of glucose were obtained in 320–350 ℃ water. In addition, below 350 ℃ the cellulose decomposition rate was slower than that of cellobiose and glucose, while above 350 ℃, the cellulose hydrolysis rate highly increased and exceeded that of the cellobiose and glucose. They suggested that intra- and intermolecular hydrogen linkages in the cellulose crystal are cleaved, and the hydrolysis of cellulose takes place with dissolution in water.

Kamio et al. (Kamio et al., 2007) investigated the liquefaction process of cellulose with subcritical water. In this study, microcrystalline cellulose degraded to oligosaccharides with a high degree of polymerization (DP), and then decomposed to

monosaccharides and pyrolysis products. In these steps, diffusion of water monomer to cellulose surface and hydrolysis reactions of water monomer with a cellulose molecule at a surface had occurred.

For lignin liquefaction analysis, liquefaction of guaiacol was carried out (Wahyudiono et al., 2007). In supercritical water, catechol, phenol, and cresol were produced as the main products of liquefaction. With an increase in the reaction time, the amount of guaiacol decreased, while the amount of derived compounds of guaiacol increased.

2.1.1.2. Woody biomass

Woody biomass, generally produced from forestry, is cellulose and lignin rich material and a promising feedstock for the HTL process. HTL of beech and spruce wood were carried out by Demirbas (Demirbas, 2005). Wood powder was liquefied in an autoclave reactor in the reaction temperature range of around 275–325 ℃ (550–650 K). The biomass to water ratio was 1 g:10 ml, and the reaction time was 25 min. In this study, the maximum liquid yield (49%) was obtained from the spruce wood powder at 320 ℃. The yield of WSF increased, but the oil phase generally decreased with the increasing lignin content of the biomass.

Karagöz et al. (Karagöz et al., 2005) investigated the distribution of products produced from the HTL process of pine wood sawdust (280 ℃ for 15 min). The highest oil yield was 8.6%, consisting mainly of 4-methylphenol, guaiacol and furfural. The major gas product was carbon dioxide.

2.1.1.3. Non-woody biomass

Yuan et al. (Yuan et al., 2009) investigated the mass balance and structure of oil and residues obtained from thermochemical conversion of non-woody biomass. Straw was hydrothermally liquefied with subcritical water at the temperature of 200, 220, 250, 300, and 310 ℃. They suggested that the main carbohydrate compounds began to decompose at 200 ℃, while the lignin decomposed between 250–300 ℃.

Hydrothermal liquefaction of dried distillers grain with soluble (DDGS) was investigated by Mørup et al. (Mørup et al., 2012). A novel stop-flow reactor system was used under different temperature ranges (300–400 ℃), fixed pressure (25 MPa), and fixed reaction time (15 min). HTL oil yields were improved, char formation decreased, and the heating values of the oil increased with higher reaction temperature.

2.1.1.4. Algal biomass

HTL is a proven method for thermochemical conversion of wet algae biomass. Various algal strains, for example, *Nannochloropsis sp*. (Rodolfi et al., 2009), *Botryococcus braunii* (Metzger & Largeau, 2005), and *Spirulina* (Vardon et al., 2011) were used in the HTL experiments. Fast and vigorous growing algae seemed suitable for HTL, thus improving the overall economic balance of the process (López Barreiro et al., 2013).

2.1.2. Process parameters

There are several factors in HTL to determine physicochemical properties of products. The competition among hydrolysis, fragmentation, or in other words, depolymerization, and repolymerization of biomass is closely related to the reaction temperature (Akhtar & Amin, 2011). Xu and Etcheverry (Xu & Etcheverry, 2008) investigated the effect of subcritical and supercritical liquefaction of Jack pine powder under a 2 MPa pressure of H_2. A 25% increase in oil yield was observed when the temperature rose from 220 to 350 ℃. The liquid production rate was higher when temperatures ranged from 250 to 300 ℃. Around 300 ℃, a decrease in the degradation rate was attributed to repolymerization and cyclization of the compounds.

Several researches have shown the effects of residence time on HTL. Optimization of residence times is important for adequate depolymerization of biomass. Many researchers have indicated that longer residence times do not increase or even suppress the oil yield (Boocock & Sherman, 1985; Yan et al., 1999; Sasaki et al., 2003).

The mass ratio of biomass in water is considered a key parameter for the liquefaction yield of hydrothermal processes. Generally, low biomass to water ratio is suitable for the production of liquids and gases, due to the denser solvent medium enhancing the extraction process. Interactions between molecules of biomass and water can inhibit dissolution of biomass components, which enhance the dissolution of organic fragments. A low biomass to water ratio condition results in the

less influential interactions (Akhtar & Amin, 2011). Boocock and Sherman, however, observed that the amount of oils decreased at very low biomass to solvent ratios (Boocock & Sherman, 1985).

2.2. Catalysts for HTL of biomass

Since catalysts play an important role in HTL, it is crucial to examining their effects and mechanism to control the overall process of HTL and properties of the products. The catalytic HTL process of biomass targets further decomposition of the main biomass constituents through dehydration, isomerization, decomposition, rearrangement, etc. (Zhou et al., 2011)

2.2.1. Alkaline catalysts

Catalytic liquefaction of pine sawdust was performed at 280 ℃ for 15 min in the alkaline solutions (NaOH, Na_2CO_3, KOH, and K_2CO_3) by Karagöz et al. (Karagöz et al., 2005) In this study, the activity of alkaline catalysts on oil yield was ranked. As a catalyst, K_2CO_3 was most effective for oil production, and other catalysts were ranked as follows: KOH> Na_2CO_3>NaOH. Phenolic compounds, for instance, 3- or 4-methylphenol and eugenol were mainly produced in this process. The base catalysts increased the water-soluble hydrocarbons and decreased solid residues or so called char.

Singh et al. (Singh et al., 2015) performed the catalytic HTL of water hyacinth at temperatures ranging from 250 to 300 ℃ under several biomass to water ratios, including 1:3, 1:6, 1:12 under various residence times (15–60 min). When KOH and K_2CO_3 were used as alkaline catalysts, they significantly increased the oil yield. With 1 N

KOH solution, a maximum oil yield of 23 wt% was observed.

Barley straw with K_2CO_3 at different temperature ranges between 280–400 ℃ was hydrothermally liquefied and compared in order to optimize its process, such as recycling water soluble fractions or reusing wastewater (Zhu et al., 2015). Results showed that relatively low temperatures were adequate for oil production: a maximum yield of 34.9 wt% was shown at 300 ℃. Organic compounds identified in HTL oil were phenolics, carboxylic acids, aldehydes, and alcohols.

2.2.2. Acid catalysts

Microalgae, *Chlorella vulgaris* and *Spirulina*, were liquefied in a high pressure batch reactor at 300 ℃ and 350 ℃ (Ross et al., 2010). Organic acids were used as catalysts, including acetic acid and formic acid. Product yields were determined and the HTL oil was analyzed for elemental content and calorific values and by GC/MS to detect organic compounds. Acetic acid was a more effective catalyst for oil production than formic acid, while oxygen content was lower when formic acid was fed. HTL oil contains 70–75% carbon, 10–16% oxygen, and 4–6% nitrogen. Higher heating value ranges from 33.4-39.9 MJ/kg. Organic compounds identified in HTL oil were aromatic hydrocarbons, such as phenol and 4-ethylphenol, nitrogen heterocycles, and long chain fatty acids.

2.2.3. Metal catalysts

Matsui et al. (Matsui et al., 1997) described a study on the liquefaction of microalgae *Spirulina* in tetralin, 1-methylnaphthalene, toluene or water under hydrogen, nitrogen, or carbon monoxide with a temperature range of 300–425 ℃. The catalyst $Fe(CO)_5$-S catalyst was used, which was developed for the liquefaction of coal. With $Fe(CO)_5$-S at 350 ℃ for 60 min in tetralin under the high pressure of 5.0 MPa, the oil yield increased from 52.3 to 66.9 wt%.

Liquefaction of avocado seeds was performed in supercritical ethanol and acetone with and without KOH or $ZnCl_2$, within temperature range of 250–290 ℃ and under high pressure in an autoclave reactor (Aysu & Durak, 2015). The highest product conversion was obtained with $ZnCl_2$ as the catalyst, with a yield of 76.9%. A comparison showed that $ZnCl_2$ was more effective than KOH at all temperatures in both solvents.

2.2.4. Other catalysts

Flax (*Linum usitatissimum* L.) straw was liquefied by Harry et al. (Harry et al., 2014). The yield of furfural was examined using a high-pressure autoclave reactor, temperature range of 175–325 ℃, a pressure of 0.1–8 MPa, retention time in the range of 0–120 min, and a biomass to water ratio of 5–20 %. For the catalyst, 0.5 g and 1.0 g of HZSM-5 was used. As a catalyst, HZSM-5 provided excellent furfural yields. Increasing the catalyst amount also increased the yield mass fraction of

furfural up to 1.9% (5.7–7.6%).

3. Materials and methods

3.1. Materials

As raw, non-woody biomass samples for this study, EFB from African oil palms (*Elaeis guineensis* Jacq.) and CCNS from coconut trees (*Cocos nucifera* L.) were used. The sample particle size was approximately 0.2–0.5 mm. Moisture contents of samples were controlled around 5 wt%. Transition metal chlorides, $CuCl_2$ (97%), $NiCl_2$ (98%), and $ZnCl_2$ (reagent grade, ≥ 98%) purchased from Sigma-Aldrich were used.

Elemental composition (carbon, hydrogen, and nitrogen) of the biomass samples was analyzed using a CHNS-932 (LECO Corp, USA) and oxygen content was calculated by difference. Holocellulose, lignin, and ash contents in biomass samples were determined according to the method presented by NREL (Sluiter et al., 2010). Inductively coupled plasma-emission spectrometer (ICP-ES) analysis was performed to quantify organic components in samples. Using a microwave, 0.5 g of samples were digested with mixtures (10 ml) of HNO_3: HCl: H_2O_2 (8: 1: 1, v/v). After digestion, the samples were diluted with deionized water to 50 ml and then filtered with a filter paper (Whatman No. 42). These were analyzed using ICPS-1000IV (Shimadzu, Japan). The chemical composition and inorganic compound composition of the samples compared to woody biomass (yellow poplar) are shown in Tables 1 and 2. Thermogravimetric analysis (TGA) was performed by a Q-5000 IR

instrument (TA Instruments, USA). Samples were heated under inert atmosphere (25 ml/min N_2 flow) at a constant heating rate of 10 ℃/min up to 800 ℃.

Table 1 Chemical composition of EFB and CCNS

	Elemental analysis (%)				Holocellulose (wt%)	Klason lignin (wt%)	Extractives (wt%)	Ash (wt%)
	C	H	N	O[a]				
EFB	45.4 ± 0.4	5.0 ± 0.2	0.6 ± 0.0	49.0 ± 0.2	70.6 ± 0.2	18.0 ± 0.2	4.6 ± 0.1	6.2 ± 0.3
CCNS	49.3 ±0.5	4.8 ± 0.5	0.1 ± 0.1	45.8 ± 1.1	72.2 ± 0.1	28.6 ± 0.4	1.2 ± 0.0	0.5 ± 0.0
YP[b]	45.8 ± 0.9	5.8 ± 0.3	0.2 ± 0.0	48.2 ± 1.2	74.0 ± 0.2	30.0 ± 0.3	-	0.5 ± 0.0

[a] By difference

[b] Data from Hwang et al. (Hwang et al., 2013)

Table 2 Major inorganic compounds in EFB and CCNS

	Inorganic compound analysis (ppm)						
	Al	Ca	Fe	K	Mg	P	Si
EFB	1760	2170	2680	11930	790	750	760
CCNS	50	150	100	1410	80	260	130
YP*	20	780	10	770	280	120	10

*Data from Eom et al. (Eom et al., 2011)

3.2. Performance process of HTL

HTL process of non-woody biomass was carried out in an autoclave reactor. The schematic diagram of the autoclave reactor is shown in Fig. 1. This device includes a furnace that can heat up to 750 ℃, a stainless steel reactor, with a volume of 500 ml, a stirrer, and water-cooling system. Before reacting, the reactor was loaded with biomass, transition metal, and deionized water in a specific ratio. Then the reactor was purged for 60 seconds with N_2 gas to remove the inside air. Reactants were mixed by the stirrer, set at 300 rpm. Reactions were operated in duplicate over a temperature range of 240–330 ℃ with a heating rate of 8 ℃/min. After reaction, the reactor was cooled at a rate of -3 ℃/min and the produced gas was vented. The reactor was then opened and the remaining mixture was washed with methylene chloride and separated with filter paper (Whatman No. 42) to isolate the liquid portion from the mixture. The liquid portion was then divided into two phases, the water phase and organic phase, which was labeled as HTL oil. The solid portion was dried, weighed, and labeled as hydrochar. The product yields were calculated using the following equations:

HTL oil yield (wt%) = $W_{oil}/W_{biomass} \times 100\%$

Hydrochar yield (wt%) = $W_{char}/W_{biomass} \times 100\%$

Gas yield (wt%) = $(W_{biomass} + W_{water} - W_{oil} - W_{char} - W_{wp})/(W_{biomass} + W_{water}) \times 100\%$

Water soluble fraction (WSF) yield (wt%) = 100% - HTL oil yield

(wt%) - hydrochar yield (wt%) - gas yield (wt%)

where $W_{biomass}$ and W_{water} are the weight of the biomass sample and solvent water. W_{oil}, $W_{char,}$ and W_{wp} are the weight of HTL oil, hydrochar, and residual water phase, respectively. Furthermore, the flow chart of this experiment is described in Fig. 2.

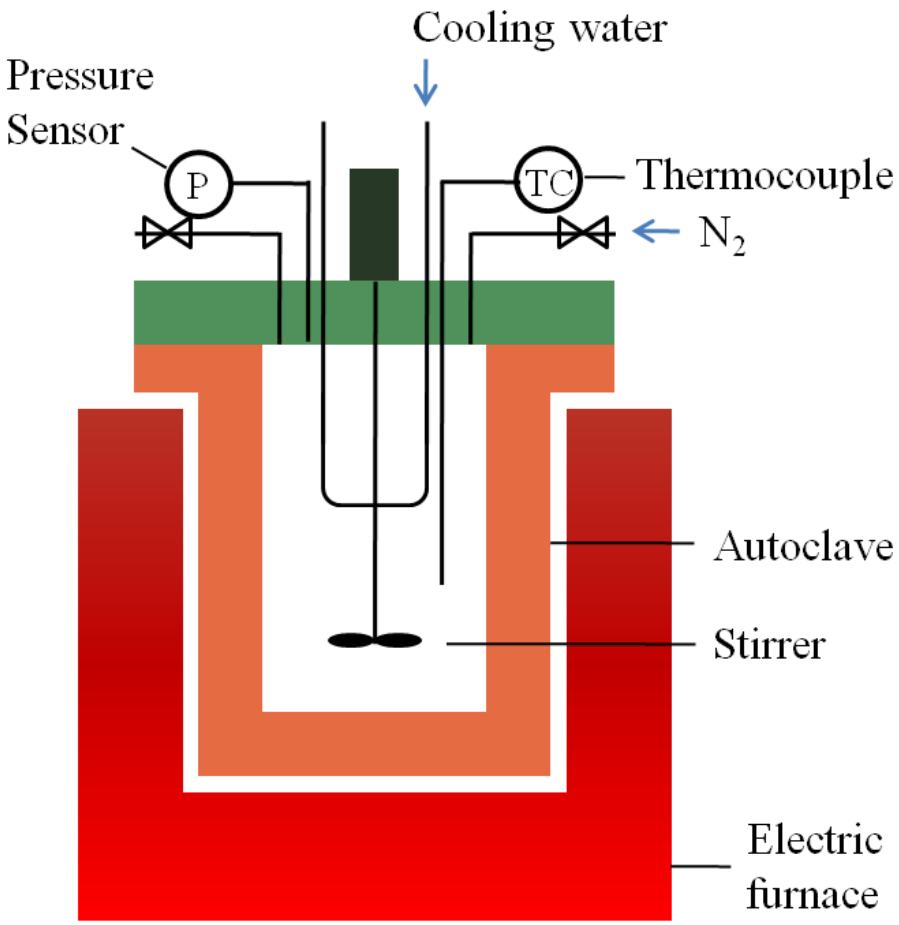

Fig. 1 Schematic diagram of autoclave reactor

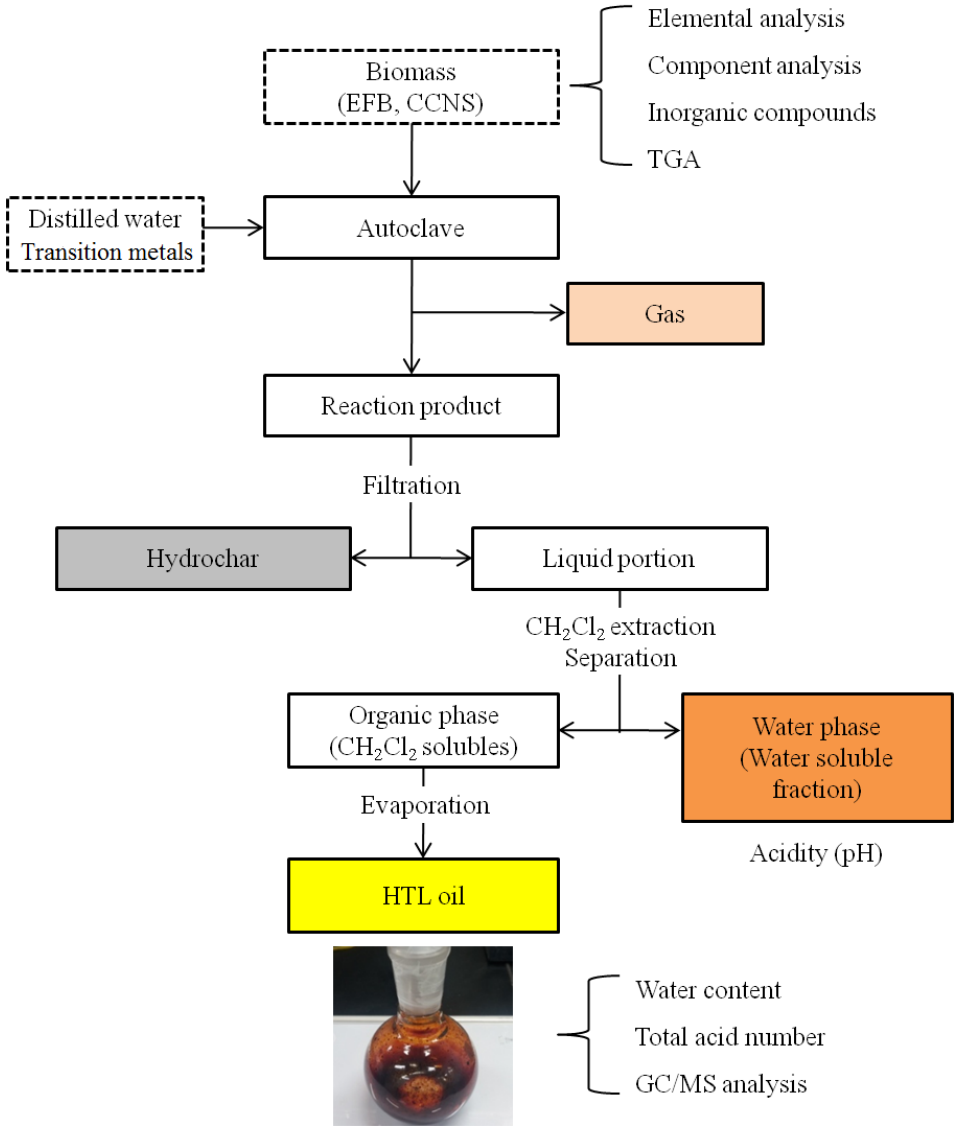

Fig. 2 Scheme of products separation and extraction

3.3. Characterization of the HTL products

3.3.1. Physicochemical analysis of HTL products

The water content of HTL oil was determined by using 870 KF Titrino plus (Radiometer, Switzerland) with HYDRANAL® -Composite 5 reagent. The acidity of HTL oil was calculated according to the method of Shao and Agblevor (Shao & Agblevor, 2015) using 848 Titrino plus (Radiometer, Switzerland). The pH of the water phase was determined using BP3001 bench top pH meter (Trans Instruments, Singapore).

3.3.2. GC/MS analysis of HTL oil

GC/MS analysis of HTL oil was performed to identify chemical compounds in HTL oil. Oil samples of 0.5 mg were diluted with 1 ml of acetone. Fluoranthene was used as an internal standard. Chemical compounds in the oil were quantified and qualified using gas chromatography mass spectrometry systems (5975C Series GC/MSD System, Agilent technologies, USA) equipped with a flame ionization detector (FID) and a DB-5 capillary column (30m x 0.25 mm x 0.25 μm). The initial oven temperature of the GC was 50 ℃ for 5min and then the temperature increased to 280 ℃ at a rate of 3 ℃/min. The injector and FID detector temperatures were 250 ℃ and 300 ℃ each. Detected chemical compounds were qualified with the NIST (National Institute of Standards and Technology) mass spectral library. Response factors (Rf) identified in a previous study (Eom et al., 2012) were used to quantify the compounds. Rf values of the other compounds were calculated roughly on the basis of their structural similarity. The concentration of each compound in HTL oil was obtained using Hwang's equation (Hwang et al., 2013).

4. Results and discussion

4.1. Characterization of the samples

As shown in Table 1, the carbon content of each biomass sample was 45.4% for EFB and 49.3 % for CCNS, whereas oxygen content was 49.0% for EFB and 45.8% for CCNS. It was noted that EFB has a greater quantity of ash and less lignin than CCNS or YP. In addition, the amount of inorganic compounds in EFB was larger than other samples.

Thermogravimetric analysis (TGA) is an analytical technique used to understand a material's thermal degradation. Fig. 3 shows dynamic TGA and derivative thermogravimetric (DTG) curves of EFB and CCNS. The first peak in the DTG (~125 ℃) corresponds to the moisture evaporation area. CCNS has two major peaks which the literature (Ramiah, 1970) shows to be related to hemicellulose and cellulose decomposition, whereas EFB has only one major peak. In addition, there is a considerable difference in the maximum degradation rate between EFB and CCNS (318.8 ℃ and 349.9 ℃, respectively). As shown in Table 2, EFB has relatively large amounts of potassium (11900 ppm) compared to CCNS (760 ppm), which catalyzes the degradation of cellulose and leads to peaks of hemicellulose and cellulose merging into one single large peak (Eom et al., 2011; Abdullah & Gerhauser, 2008). This could account for the presence of a single main peak and relatively low degradation rate temperature of

EFB. Lignin decomposition occurred under a wide temperature range of 200–700 ℃.

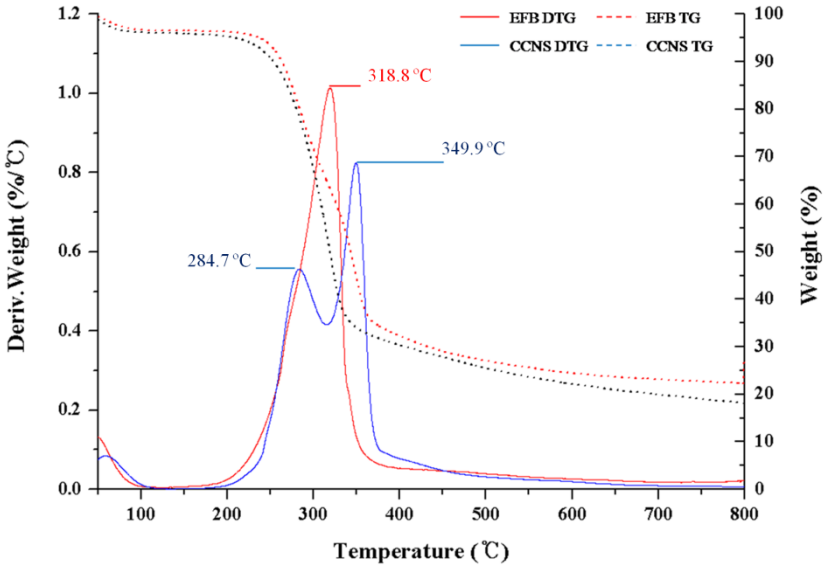

Fig. 3 TG and DTG curves of EFB and CCNS

4.2. Effect of process parameters on the HTL

4.2.1. Effect of temperature

4.2.1.1. Mass balance

The effect of temperature was studied at various intervals (240, 270, 300, and 330 ℃ with 30 min of residence time and 1:10 of biomass to deionized water ratio. Figs. 4 and 5 show the mass distribution of products obtained from HTL of EFB and CCNS.

As expected, mass composition of HTL products was affected by reaction temperature. The yield of HTL oil, the target product of this experiment, gradually increased up to 300 ℃, and then decreased slightly at 330 ℃. The highest HTL oil yields from EFB and CCNS were all obtained at 300 ℃ (22.8% and 13.9%, respectively). On the other hand, gas yields decreased at all reaction temperatures up to 330 ℃. With the rising temperature, the gas yields from EFB and CCNS decreased from 19.2% and 24.1% at 240 ℃ to 10.2% and 19.2% at 330 ℃, respectively. The yield of hydrochar showed a different decreasing trend with rising temperatures. At temperatures in the range of 240-270 ℃, the formation of hydrochar drastically decreased from 50.6 % and 52.6 % to 29.1 % and 41.5 %, respectively. Next, the yields of hydrochar gradually decreased down to 330 ℃. At 240 ℃, both yields of hydrochar were higher than 50 wt% due to incomplete degradation of cellulose (Rogalinski et al., 2008). In addition, it is shown that the

yields of WSF were in inverse proportion to the yields of hydrochar. Ultimately, clear inverse proportions of hydrochar and WSF, HTL oil and gas from each sample were found.

On equal conditions, the yield of HTL oil from EFB was significantly higher than that of CCNS. Furthermore, the yield of hydrochar from EFB was also harshly decreased compared to that of CCNS. It has been reported that alkali salts act as catalysts, increasing the amount of liquid products of HTL and suppressing char formation (Toor et al., 2011). Numerous studies show that the presence of potassium salts, such as KOH or K_2CO_3, catalyze water-gas shift reaction during HTL, increasing oil products and decreasing solid residue (Akhtar et al., 2010; Karagoz et al., 2006). Moreover, lignin polymers are prone to interact with alkali. We assumed that the potassium in EFB and CCNS accelerated the water-gas shift reaction, lignin degradation, and suppressed polymerization of biomass monomers. The difference of oil and char yield between the two samples suggests that it is due to the difference in the potassium concentration.

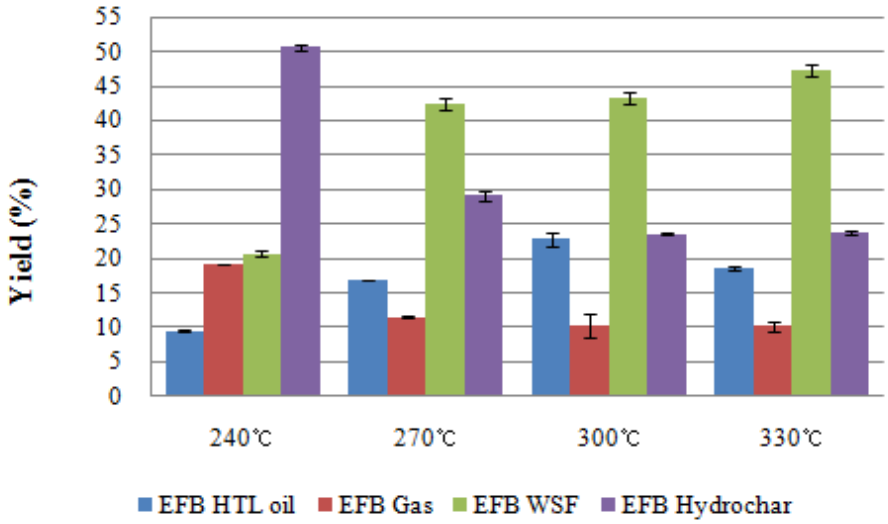

Fig. 4 Mass balance of HTL products from EFB under different temperatures

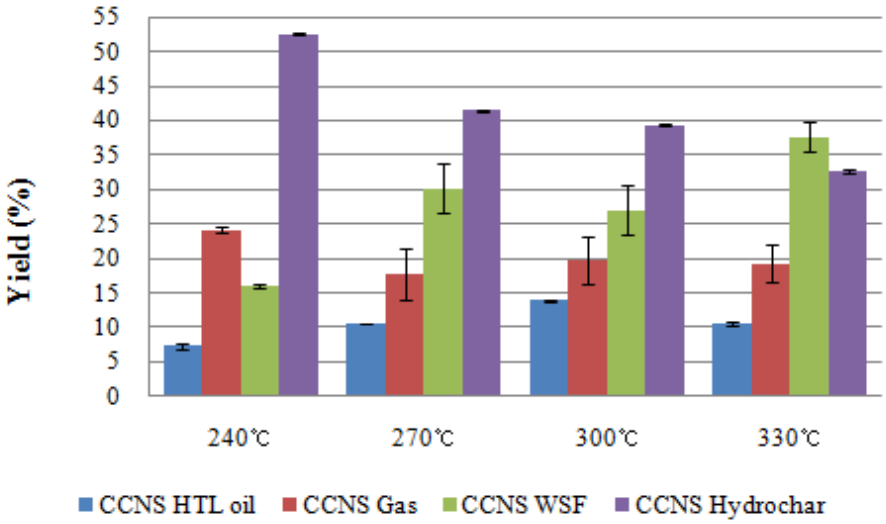

Fig. 5 Mass balance of HTL products from CCNS under different temperatures

4.2.1.2. Physicochemical properties

Physicochemical properties of HTL oil (water content, total acid number (TAN)) and water phase (pH) from EFB and CCNS are illustrated in Table 3. Water content of the samples ranged from 2.0 to 9.6%. The highest water content of HTL oil from the biomass, at 9.6%, was obtained for CCNS at 240 ℃. Water content decreased down to 300 ℃, and then increased slightly at 330 ℃. At 240 ℃, HTL oil had relatively high concentrations of aldehydes or ketones (Table 4), which can be easily converted to the hydrated form and contribute to levels of moisture (Lu et al., 2009). The relatively rapid decrease of water content in HTL oil from CCNS can be explained by change of compound concentration. The TAN value of HTL oil ranged from 110 to 240 mg KOH/g for EFB and from 98 to 189 mg KOH/g for CCNS. Acetic acid and various phenolic compounds have an effect on TAN value of the oil (Oasmaa et al., 2010). As the temperature increases, those compounds would be produced in large amounts by hydrolysis and further hydration (Table 4).

The water phase became acidic during HTL due to the WSF, such as acids, water-soluble hydrocarbons, and carbohydrates. There was a small difference between pH values in each sample under various temperatures. The water phase from EFB, however, was less acidic than that of CCNS as a result of the concentration of inorganic compounds which act as base.

Table 3 Physical properties of HTL oils under various reaction temperatures

		HTL oil		pH of water phase
		Water content (%)	TAN (mg KOH/g oil)	
EFB	240 ℃	5.6 ± 1.1	110	3.72
	270 ℃	3.5 ± 0.2	163	3.67
	300 ℃	2.0 ± 0.1	240	3.71
	330 ℃	3.6 ± 0.2	203	3.92
CCNS	240 ℃	9.6 ± 0.5	98	2.69
	270 ℃	6.5 ± 0.3	190	2.78
	300 ℃	3.3 ± 0.1	189	2.75
	330 ℃	4.9 ± 0.3	180	2.90

4.2.1.3. GC/MS analysis

The chemical composition of HTL oil was characterized by GC/MS analysis, and the organic components are listed in Tables 4 and 5. In addition, their chromatograms are illustrated in Figs. 6 and 7. In EFB HTL oil, 18 phenolic compounds were identified, and phenol (7), cresol (11, 12, 13), guaiacol (14), syringol (19), syringyl acetone (28) were the major compounds. It was reported that phenolic compounds were created by lignin degradation, such as hydrolysis and further hydration to form hydrolated benzenes or alkylated benzenes (Barbier et al., 2012). We, therefore, classified those phenolics as lignin-derived compounds. From the carbohydrates, 10 compounds were detected, for example, acetic acid (1), furfural (3), and various cyclic compounds (4, 5, 6, 8, 9, 10, and 16). In CCNS HTL oil, 17 lignin-derived compounds and 7 carbohydrates were found.

As shown in Figs. 8 and 9, the total amount of chemical compounds in HTL oil from EFB increased until 300 ℃, and then decreased slightly at 330 ℃. In the case of CCNS, the total amount of compounds at 300 ℃ was similar to the amount at 330 ℃. It could be explained by the fact that the amount of holocellulose-derived carbohydrates was maximized at 300 ℃, whereas lignin-derived compounds gradually increased with a rise in temperature. On the other hand, the ratio of the amount of acids and aldehydes to the total amount of chemical compounds decreased as temperature increased. The concentration of ketones and lignin-derived compounds, however, increased as the temperature rose.

Table 4 Quantitative analysis of chemical compounds in the HTL oil from EFB under different temperatures

Peak no.	Compound	Source	Relative amount (area / IS area)			
			240 ℃	270 ℃	300 ℃	330 ℃
1	Acetic acid	C[a]	2.09	2.57	3.10	2.25
2	2,3-Dihydrofuran	C	-	-	0.43	0.21
3	Furfural	C	1.82	1.18	0.99	0.56
4	3-Methyl-2-cyclopentenone	C	-	0.25	1.32	1.24
5	*trans*-1,2-Cyclopentanediol	C	-	-	0.05	-
6	1,2-Cyclopentanedione	C	-	0.09	0.24	0.05
7	Phenol	L[b]	1.65	1.82	2.53	2.17
8	3,4-Dimethyl-2-Cyclopentenone	C	-	0.01	0.17	0.06
9	3-Methyl-1,2-cyclopentanedione	C	0.42	0.92	0.60	-
10	2,3-Dimethyl-2-cyclopentenone	C	-	0.08	0.37	0.50
11	*m*-Cresol	L	-	-	0.04	-
12	*o*-Cresol	L	-	-	-	0.04
13	*p*-Cresol	L	-	-	0.07	-
14	Guaiacol	L	0.19	0.42	1.24	1.53
15	4-Ethylphenol	L	-	0.04	-	-
16	2-Acetonylcyclopentanone	C	-	-	0.09	0.12
17	Creosol	L	-	-	0.13	0.22
18	4-Ethylguaiacol	L	-	-	0.47	0.44
19	Syringol	L	0.18	0.54	1.30	1.46
20	4-Propylguaiacol	L	-	-	0.09	0.09
21	Vanillin	L	0.03	0.06	-	-
22	Isovanillic acid	L	-	-	0.21	0.29
23	4-Ethylsyringol	L	-	0.07	0.21	0.19
24	Guaiacylacetone	L	0.03	0.05	0.12	-
25	4-Propylsyringol	L	-	-	0.19	0.20
26	Syringaldehyde	L	0.08	0.09	0.08	0.09
27	Acetosyringone	L	-	-	0.06	-
28	Syringyl acetone	L	0.12	0.22	0.38	0.20
	Sum of carbohydrates		4.33	5.11	7.37	4.97
	Sum of Lignin-derived compounds		2.29	3.31	7.11	6.91
	Total		6.62	8.42	14.48	11.89

[a] Carbohydrates
[b] Lignin-derived compounds

Table 5 Quantitative analysis of chemical compounds in the HTL oil from CCNS under different temperatures

Peak no.	Compound	Source	Relative amount (area / IS area)			
			240 ℃	270 ℃	300 ℃	330 ℃
1	Acetic acid	C	0.37	0.87	1.46	0.73
2	2,3-Dihydrofuran	C	-	-	0.13	0.73
3	Furfural	C	4.15	3.89	6.08	4.14
4	3-Methyl-2-cyclopentenone	C	-	1.08	0.17	1.14
5	1,2-Cyclopentanedione	C	-	-	0.55	0.60
6	Phenol	L	1.14	2.69	4.79	5.99
7	3-Methyl-1,2-cyclopentanedione	C	0.03	-	0.74	0.32
8	2,3-Dimethyl-2-cyclopentenone	C	-	-	0.20	0.36
9	Guaiacol	L	0.22	1.60	2.07	2.58
10	Creosol	L	-	-	0.18	0.77
11	4-Ethylguaiacol	L	-	-	0.46	0.68
12	Syringol	L	0.11	0.86	1.56	1.83
13	4-Propylguaiacol	L	-	-	0.09	0.11
14	Vanillin	L	0.07	0.29	0.29	-
15	Isovanillic acid	L	-	-	0.22	0.40
16	Isoeugenol	L	-	-	0.12	-
17	Apocynin	L	-	-	0.19	-
18	4-Ethylsyringol	L	-	-	0.19	0.24
19	Guaiacylacetone	L	0.04	0.22	0.33	0.18
20	4-Propylsyringol	L	-	-	0.15	0.12
21	Syringaldehyde	L	-	0.05	0.28	0.12
22	Acetosyringone	L	-	-	0.14	-
23	Syringyl acetone	L	-	0.10	0.40	0.14
24	4-Allylsyringol	L	-	-	0.18	-
	Sum of carbohydrates		4.55	5.85	9.33	8.01
	Sum of Lignin-derived compounds		1.57	5.80	11.63	13.16
	Total		6.12	11.65	20.96	21.17

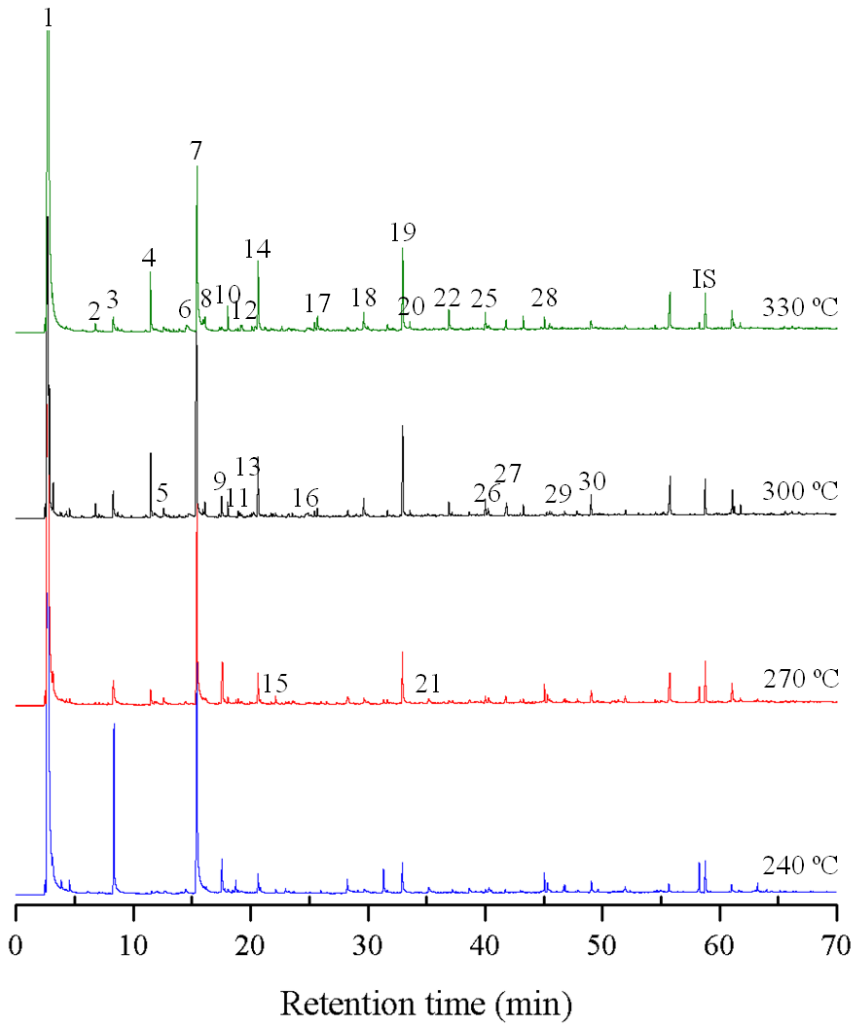

Fig. 6 Gas chromatogram of chemical compounds in HTL oil from EFB

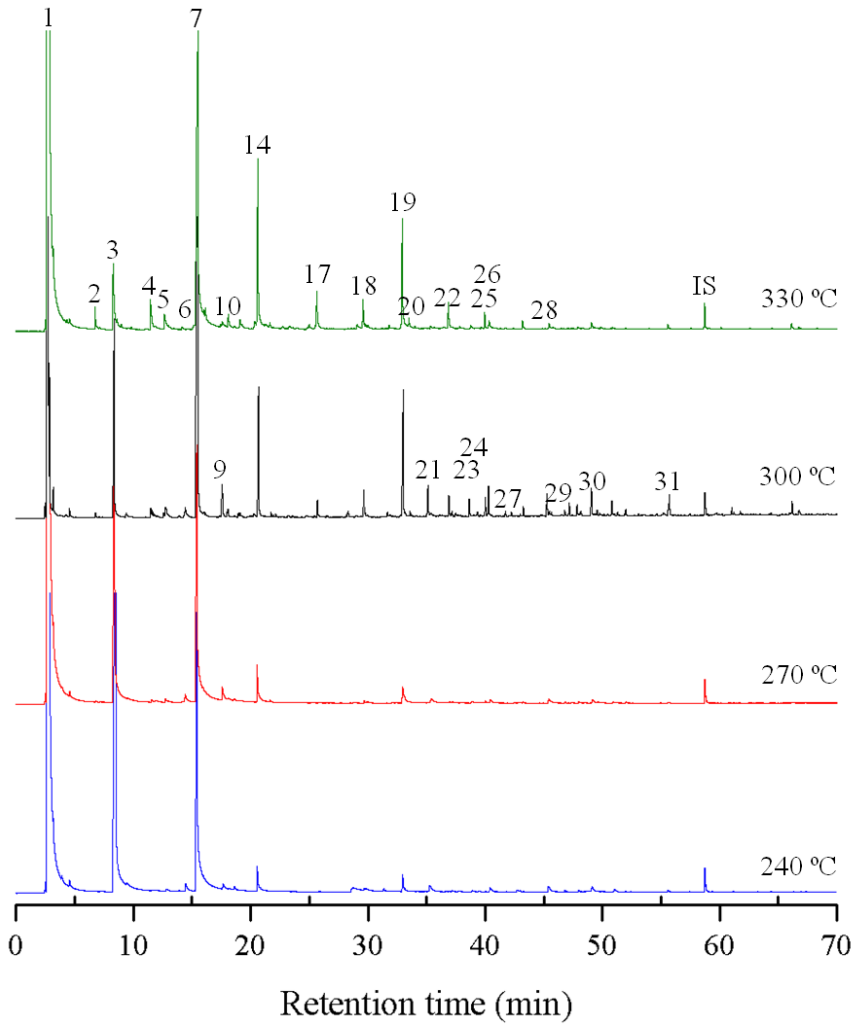

Fig. 7 Gas chromatogram of chemical compounds in HTL oil from CCNS

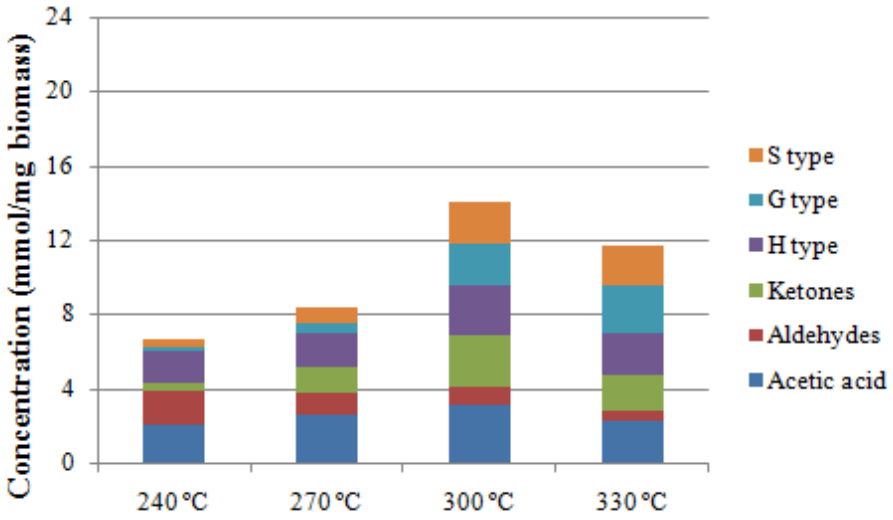

Fig. 8 Amount of different chemical compound groups in HTL oil from EFB at various temperatures

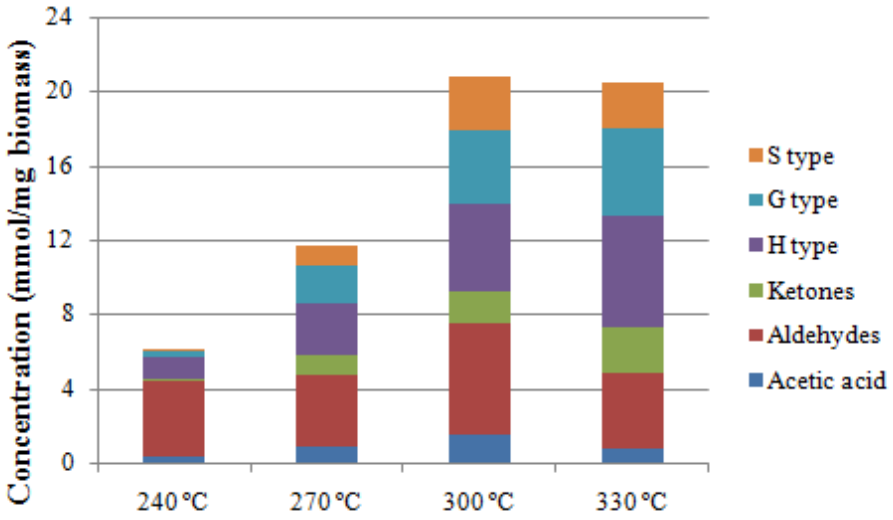

Fig. 9 Amount of different chemical compound groups in HTL oil from CCNS at various temperatures

4.2.2. Effect of transition metal chlorides

4.2.2.1. Mass balance

The catalytic effect on HTL was investigated at 300 ℃ and 30 min of residence time using transition metal chlorides ($ZnCl_2$, $CuCl_2$, and $NiCl_2$). The effect of transition metal concentration was also studied by adding 2.5%, 5.0%, and 10.0% metals.

The effect of transition metal chlorides on the mass balance of products obtained from HTL of EFB is shown in Fig. 10. In the presence of $ZnCl_2$ (Fig. 10A), a harsh decrease in the HTL oil yields was observed. The HTL oil showed relatively low yields in the range of 10.6–14.1%, by increasing metal loading from 2.5 to 10.0%. The oil yield dramatically reduced with the presence of the metals, but the dosage had a relatively small effect on it. In addition, gas increased between 12.1% and 15.7%, and the yield of EFB hydrochar rose from 23.6 to 31.6% with increasing metal concentrations from 0 to 10.0%. No critical change with the metals was observed in the yield of WSF. While in the presence of $CuCl_2$ (Fig. 10B), a similar trend was found in $ZnCl_2$, but a much more significant change was detected: the yield of HTL oil decreased (4.5–10.2%) and hydrochar increased (33.5–40.7%). The gas yield sharply rose (19.7–23.4%) but WSF decreased (32.6–35.5%), unlike that of $ZnCl_2$. Furthermore, $NiCl_2$ also affected the yield of HTL products (Fig. 10C). HTL oil decreased (8.9–12.2%), gas and hydrochar increased (13.9–21.4% and 25.4–33.2%, respectively).

Fig. 11A shows the effect of $ZnCl_2$ on the mass balance of products

obtained from HTL of CCNS. The yield of HTL oil from CCNS decreased, ranging from 5.6% to 6.5%, compared to those of obtained by HTL without transition metals. However, gas yield decreased in the range of 10.9–16.4%. The change in the amount of hydrochar was fairly stable by increasing metal concentration, whereas WSF dramatically increased by the presence of the metal. Similar trends of mass balance were seen in catalytic HTL products with $CuCl_2$ and $NiCl_2$ (Figs. 11B and 11C).

The decrease in HTL oil yields in the transition metal chlorides can be explained by catalytic cracking reactions. The transition metal chloride as salt is a weak base and a strong acid, so it becomes acidic in water. Under acidic conditions, liquid products are fragmented, converted to gaseous or hydrophilic WSF, or undergo repolymerization to become hydrochar (Zhou et al., 2011). At 300 ℃, the highest liquid oil yield from HTL of cellulose in acid (pH 3) was reported (Yin & Tan, 2012). Our study, however show that yield of liquid oil from HTL of biomass under acidic conditions was even lower than that of neutral conditions. We can therefore infer that non-cellulosic compounds in EFB and CCNS encourage further reactions (both depolymerization and repolymerization) of cellulose-derived hydrocarbons. In addition, we can assume that compositional differences between the feedstock or the kinds of transition metal chlorides used, are the important factors of the mass distribution of products.

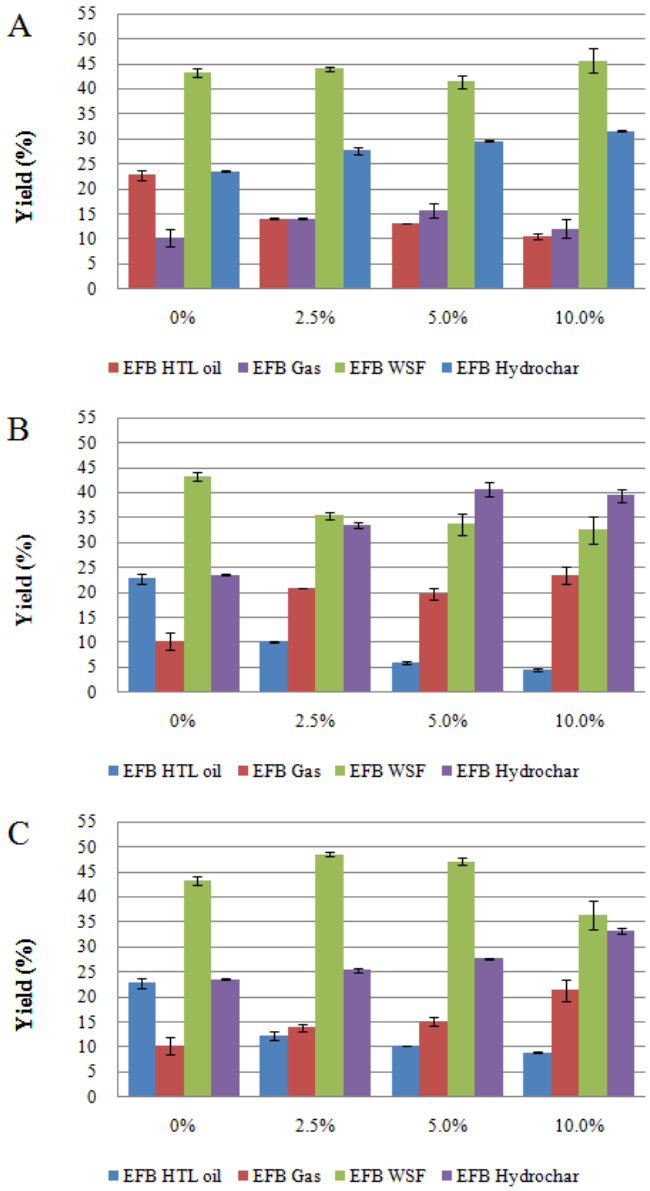

Fig. 10 Mass balance of HTL products from EFB under different conditions (A: $ZnCl_2$, B: $CuCl_2$, C: $NiCl_2$)

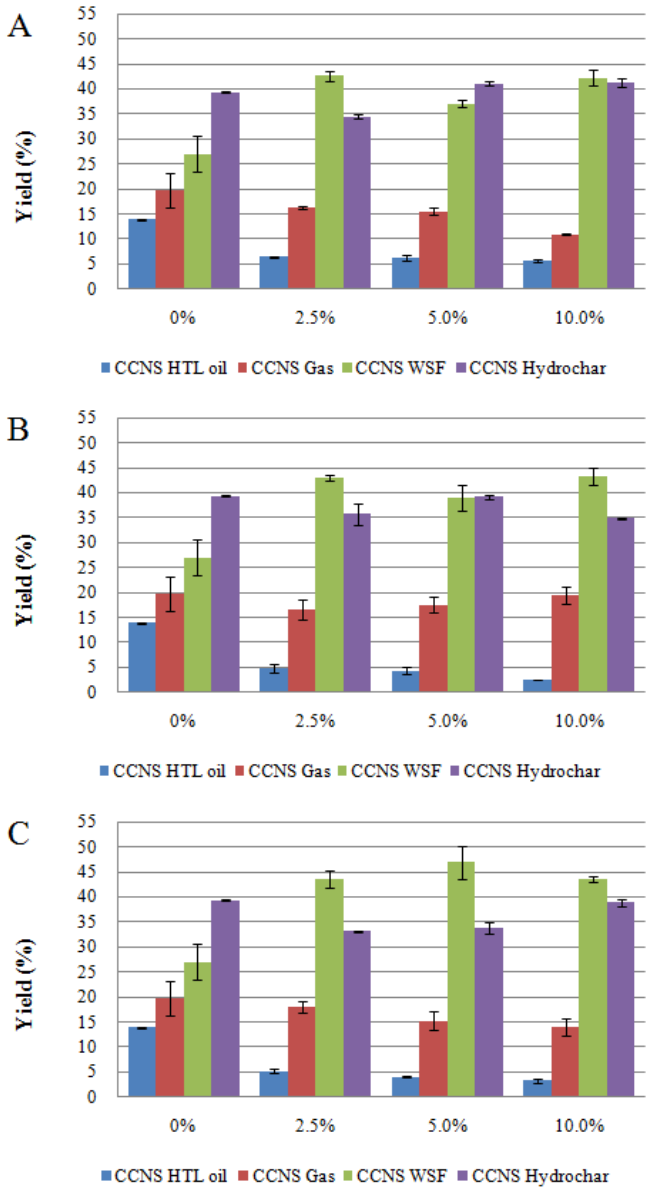

Fig. 11 Mass balance of HTL products from CCNS under different conditions (A: $ZnCl_2$, B: $CuCl_2$, C: $NiCl_2$)

4.2.2.2. Physicochemical properties

Table 6 illustrates physicochemical properties of HTL oil and the water phase from EFB and CCNS in the presence of transition metals. Water content of HTL oil rose by increasing metal loading from 2.5 to 10.0%. In both cases of EFB and CCNS, transition metal chlorides increased water content of HTL oil. Above all, $CuCl_2$ greatly affected the water content, with an increase in the range of 5.8–10.0% for EFB, while that of non-catalytic was 2.0%. The TAN value of HTL oil drastically increased compared to the control when 2.5% of the transition metal was loaded. The value, however, decreased with use of 5.0–10.0% catalyst, even lower than that of the control.

The water phase became far more acidic when the transition metal chlorides were used. The more metals were loaded, the more acidic the water phase was. As aforementioned, transition metal chloride, itself, becomes acidic in water due to the chloride ions. In addition, under acidic conditions, more cellulose-derived compounds are produced which may affect the acidity of the water phase. Similar to the results with pure water, the water phase from CCNS was more acidic than that of EFB. In addition, under $NiCl_2$ conditions, the water phase showed the lowest pH value.

Table 6 Physical properties of HTL oils with various transition metal chlorides at 300 ℃ and 30 min of reaction time

			HTL oil		pH of water phase
			Water content (%)	TAN (mg KOH/g oil)	
EFB	$ZnCl_2$	2.5%	3.0 ± 0.6	328	3.21
		5.0%	3.6 ± 0.5	179	2.95
		10.0%	4.6 ± 0.1	154	2.70
	$CuCl_2$	2.5%	6.5 ± 0.2	292	3.08
		5.0%	5.8 ± 0.5	201	2.75
		10.0%	10.0 ± 0.4	195	2.30
	$NiCl_2$	2.5%	2.6 ± 0.4	251	3.16
		5.0%	3.1 ± 0.5	197	2.99
		10.0%	4.5 ± 0.3	209	2.67
CCNS	$ZnCl_2$	2.5%	6.4 ± 0.8	167	2.44
		5.0%	6.5 ± 0.5	127	2.38
		10.0%	7.5 ± 0.4	115	2.19
	$CuCl_2$	2.5%	4.2 ± 0.5	205	2.27
		5.0%	7.5 ± 0.5	144	2.36
		10.0%	11.8 ± 1.1	126	2.05
	$NiCl_2$	2.5%	5.1 ± 0.1	220	2.21
		5.0%	4.5 ± 0.7	168	2.12
		10.0%	8.4 ± 0.5	179	2.00

4.2.2.3. GC/MS analysis

The chemical composition of catalytic HTL oil from EFB and CCNS was characterized by GC/MS analysis, and the organic components are listed in Tables 7 and 8, respectively. Chromatograms of chemical compounds with using 10% of transition metals are illustrated in Figs. 12 and 13.

More than 20 compounds were detected in HTL oil from EFB with $ZnCl_2$. By comparison, with non-catalytic oil, quantified amounts of acetic acid increased drastically in the presence of $ZnCl_2$, but there is a high probability of peak overlapping by unidentified compounds. There was little difference of holocellulose-derived compounds (except acetic acid) between the control and the oil with $ZnCl_2$. The lignin-derived compounds, however, gradually decreased with increasing amounts of catalyst (Fig. 14). Because lignin is apt to interact with alkali, it does not readily interact with acid (Zhou et al., 2011). With $CuCl_2$ and $NiCl_2$, similar trends of increasing carbohydrates and decreasing lignin-derived compounds were shown. $CuCl_2$ showed the lowest lignin-derived concentration, while $NiCl_2$ showed the lowest carbohydrates concentration. It is reported that hydration products such as formic acid or levulinic acid, and dehydration products, such as 1, 2, 4-benzentriol were produced during acidic HTL (Yin & Tan, 2012). In HTL oil with $CuCl_2$, levulinic acid (hydration product) and 2-Methoxy-1, 4-benzenediol (dehydration product) were found.

HTL oil from CCNS with $ZnCl_2$ showed more than 20 peaks. The concentration of acetic acid became much lower. Both carbohydrates

and lignin-derived compounds were gradually decreased with increasing amounts of metal, this was especially true for aldehyde (mainly furfural) and H type phenolic compounds, which severely decreased (Fig. 15). With $CuCl_2$ and $NiCl_2$, the same concentration change was found. As shown in Fig. 13, very small lignin-derived compound peaks were detected in the presence of $CuCl_2$. In the case of $NiCl_2$, all the peaks, except furfural and guaiacol, became smaller.

In the presence of all the metal catalysts, ɣ-valerolactone (GVL) was identified in HTL oil only in the presence of these catalysts. GVL is known to be produced via hydrogenation of levulinic acid over a non-acidic catalyst at mild temperature conditions (Serrano-Ruiz et al., 2012). It is also known that levulinic acid is produced by hydrothermal decomposition of cellulose, especially under acidic conditions (Möller et al., 2013; Yin & Tan, 2012). It is assumed that levulinic acid, which was detected in HTL oil from both feedstocks with $CuCl_2$, is hydrogenated at high temperature conditions undeterred by acidity, leading to the production of GVL. Interestingly, unlike $ZnCl_2$ and $NiCl_2$, in the presence of $CuCl_2$ relatively small amounts of GVL and large amounts of levulinic acid were detected. We suggest that Cu^{2+} from $CuCl_2$ disrupted the hydrogenation of levulinic acid, resulting in much of the levulinic acid remaining in the HTL oil. The proposed pathway of acidic hydrothermal decomposition of cellulose with transition metal chloride catalysts is shown in Fig. 16. In addition, identified mass peaks of GVL and levulinic acid compared with the data from NIST (National Institute of Standards and Technology) mass spectral library are shown in Figs. 17 and 18.

Table 7 Quantitative analysis of chemical compounds in the HTL oil from EFB over various transition metal chloride concentrations (300 ℃, 30 min of reaction time)

Peak no.	Compound	Source	Concentration (mg/g biomass)									
			Control	ZnCl2			CuCl2			NiCl2		
				10.0%	5.0%	2.5%	10.0%	5.0%	2.5%	10.0%	5.0%	2.5%
1	Acetic acid	C	3.10	2.77	7.10	8.15	1.47	5.00	7.24	2.15	5.99	6.03
2	2,3-Dihydrofuran	C	0.43	0.23	0.27	0.23	0.18	0.23	0.18	0.10	0.17	0.18
3	Furfural	C	0.99	1.58	1.60	0.87	2.92	3.05	1.39	1.52	0.80	0.85
4	3-Methyl-2-cyclopentenone	C	1.32	0.52	0.87	0.95	0.19	0.41	0.61	0.42	0.56	0.70
5	*trans*-1,2-Cyclopentanediol	C	0.05	0.07	-	-	0.03	0.08	0.00	0.08	-	-
6	1,2-Cyclopentanedione	C	0.24	0.16	0.16	0.09	0.24	0.61	0.28	0.20	0.05	0.17
7	γ-Valerolactone	C	-	0.18	0.10	-	0.09	-	-	0.40	0.18	0.10
8	Phenol	L	2.53	1.87	2.64	2.31	1.97	3.14	2.47	1.99	2.19	2.31
9	3,4-Dimethyl-2-Cyclopentenone	C	0.17	0.16	0.35	0.38	0.05	0.17	0.33	0.05	0.25	0.26
10	3-Methyl-1,2-cyclopentanedione	C	0.60	0.19	0.21	0.20	0.12	0.07	0.37	0.22	-	-
11	2,3-Dimethyl-2-cyclopentenone	C	0.37	0.25	0.35	0.31	0.13	0.22	0.24	0.22	0.27	0.25
12	*m*-Cresol	L	0.04	-	-	-	-	-	-	-	-	-
13	*o*-Cresol	L	-	-	-	-	0.01	-	-	0.01	-	-
14	*p*-Cresol	L	0.07	0.04	-	-	-	-	-	0.06	-	
15	Levulinic acid	C	-	-	-	-	0.83	0.26	-	-	-	-
16	Guaiacol	L	1.24	1.09	1.69	1.68	0.96	1.58	1.44	0.97	1.31	1.27
17	4-Ethylphenol	L	-	-	-	-	0.02	-	-	0.04	-	-
18	Benzoic acid	L	-	0.06	-	-	-	-	-	0.13	-	-
19	2-Acetonylcyclopentanone	C	0.09	-	-	-	-	-	-	-	-	-
20	Creosol	L	0.13	0.07	0.08	-	-	-	-	0.06	-	-
21	2-Methoxy-1,4-benzenediol	L	-	-	-	-	0.07	-	-	-	-	-
22	4-Ethylguaiacol	L	0.47	0.06	0.16	0.19	0.04	0.03	0.11	0.19	0.12	0.15
23	Syringol	L	1.30	0.91	1.37	1.35	0.18	0.86	1.13	0.49	0.87	0.99
24	4-Propylguaiacol	L	0.09	-	-	-	-	-	-	-	-	-
25	Vanillin	L	-	-	-	-	0.02	-	-	-	-	-
26	Isovanillic acid	L	0.21	0.08	0.13	0.14	-	0.05	0.11	0.04	0.06	0.10
27	4-Ethylsyringol	L	0.21	0.07	0.13	0.14	-	-	0.10	0.04	0.08	0.12
28	Guaiacyl acetone	L	0.12	0.09	-	-	0.12	0.08	0.00	0.12	0.07	0.07
29	4-Propylsyringol	L	0.19	-	0.07	0.09	-	-	-	-	-	0.07
30	Syringaldehyde	L	0.08	-	-	-	-	-	-	-	-	-
31	Acetosyringone	L	0.06	-	-	-	0.05	0.05	-	-	-	-
32	Syringyl acetone	L	0.38	0.23	0.20	0.26	0.12	0.11	0.12	0.19	0.11	0.13
Sum of carbohydrates			7.37	6.11	11.01	11.18	6.25	10.11	10.63	5.35	8.28	8.54
Sum of Lignin-derived compounds			7.11	4.57	6.46	6.15	3.57	5.91	5.48	4.33	4.82	5.22
Total			14.48	10.68	17.46	17.33	9.82	16.03	16.11	9.68	13.10	13.75

Table 8 Quantitative analysis of chemical compounds in the HTL oil from CCNS over various transition metal chloride concentrations (300 ℃, 30 min of reaction time)

Peak no.	Compound	Source	Concentration (mg/g biomass)									
			Control	ZnCl2			CuCl2			NiCl2		
				10.0%	5.0%	2.5%	10.0%	5.0%	2.5%	10.0%	5.0%	2.5%
1	Acetic acid	C	1.46	0.29	0.29	0.49	0.13	0.37	0.49	0.24	0.20	0.28
2	2,3-Dihydrofuran	C	0.13	0.12	0.15	0.25	-	0.49	0.27	0.33	0.06	0.23
3	Furfural	C	6.08	1.72	4.33	7.30	1.71	5.13	6.76	4.36	2.70	2.41
4	3-Methyl-2-cyclopentenone	C	0.17	0.05	0.11	0.19	0.06	0.16	0.13	0.23	0.12	0.12
5	1,2-Cyclopentanedione	C	0.55	0.06	0.38	0.64	0.04	0.17	0.61	0.35	0.31	0.38
6	ɣ-Valerolactone	C	-	0.06	0.14	0.23	0.05	0.07	-	0.32	0.28	0.32
7	Phenol	L	4.79	2.07	3.77	6.35	3.62	5.04	5.14	2.40	3.53	3.65
8	3-Methyl-1,2-cyclopentanedione	C	0.74	0.09	0.18	0.30	-	-	0.18	0.21	0.18	0.15
9	2,3-Dimethyl-2-cyclopentenone	C	0.20	-	0.13	0.22	0.12	0.15	0.22	0.26	0.16	0.15
10	Levulinic acid	C	-	-	-	-	1.97	1.37	0.32	-	-	-
11	Guaiacol	L	2.07	1.55	1.85	1.98	0.15	0.16	0.95	1.86	2.14	2.56
12	4-Ethylphenol	L	-	-	-	-	0.03	-	-	-	-	-
13	Creosol	L	0.18	0.03	0.08	0.13	-	-	-	0.06	0.07	0.07
14	4-Ethylguaiacol	L	0.46		0.05	0.09	0.14	0.21	0.23	0.03	0.08	0.05
15	Syringol	L	1.56	0.51	1.00	1.19	0.01	0.14	0.48	0.26	0.49	0.73
16	4-Propylguaiacol	L	0.09	-	0.03	0.04	-	-	-	-	-	-
17	Vanillin	L	0.29	-	0.05	0.09	-	-	-	-	-	-
18	Isovanillic acid	L	0.22	-	0.06	0.10	-	-	-	-	0.03	0.04
19	Isoeugenol	L	0.12	-	-	-	-	-	-	-	-	-
20	Apocynin	L	0.19	-	0.06	0.10	-	-	-	-	-	-
21	4-Ethylsyringol	L	0.19	-	0.04	0.06	-	-	-	-	-	-
22	Guaiacylacetone	L	0.33	0.10	0.15	0.25	-	-	-	0.10	0.15	0.19
23	4-Propylsyringol	L	0.15	-	0.05	-	-	-	-	-	-	-
24	Syringaldehyde	L	0.28	-	-	0.09	-	-	-	-	-	-
25	Acetosyringone	L	0.14	-	0.02	0.04	-	-	-	-	-	-
26	Syringyl acetone	L	0.40	0.06	0.11	0.19	-	-	-	-	0.07	0.10
27	4-Allylsyringol	L	0.18	-	0.05	0.09	-	-	-	-	-	-
Sum of carbohydrates			9.33	2.40	5.71	9.61	4.07	7.90	9.00	6.29	4.01	4.04
Sum of Lignin-derived compounds			11.63	4.31	7.37	10.79	3.94	5.54	6.80	4.71	6.14	7.39
Total			20.96	6.72	13.08	20.40	8.01	13.45	15.79	11.00	10.16	11.43

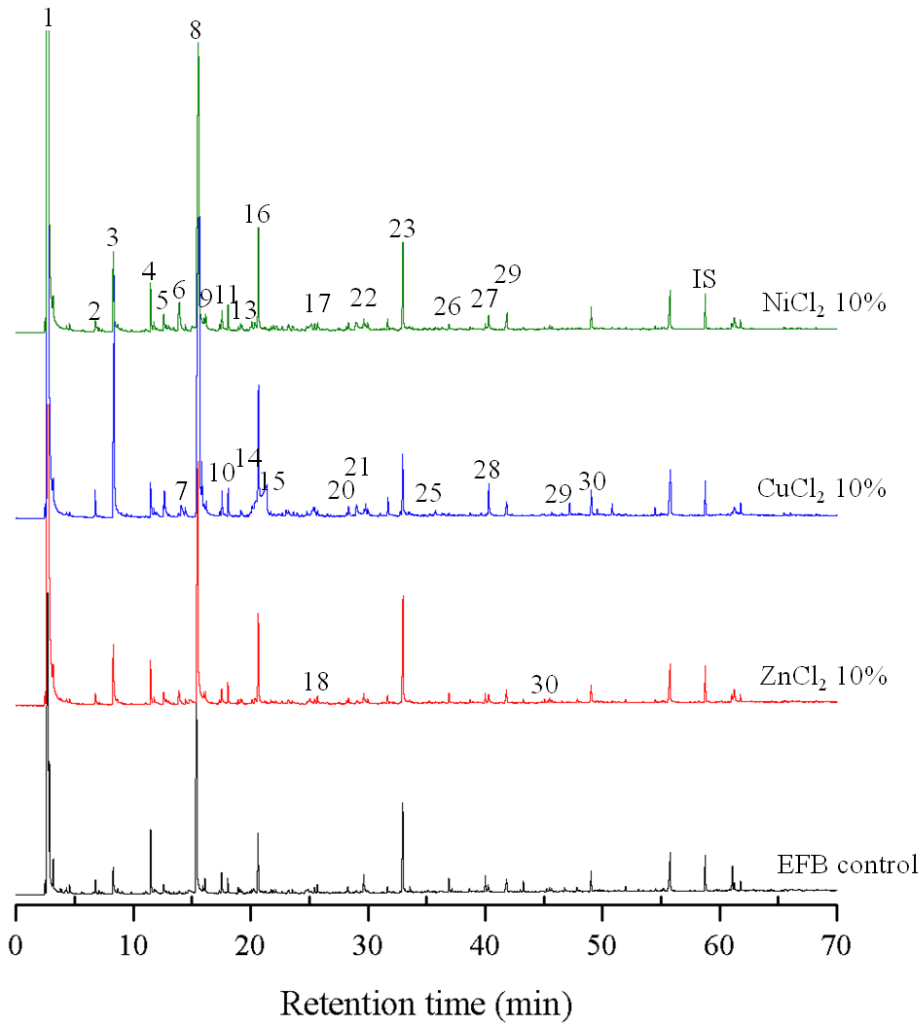

Fig. 12 Gas chromatogram of chemical compounds in HTL oil from EFB with use of various transition metal chlorides

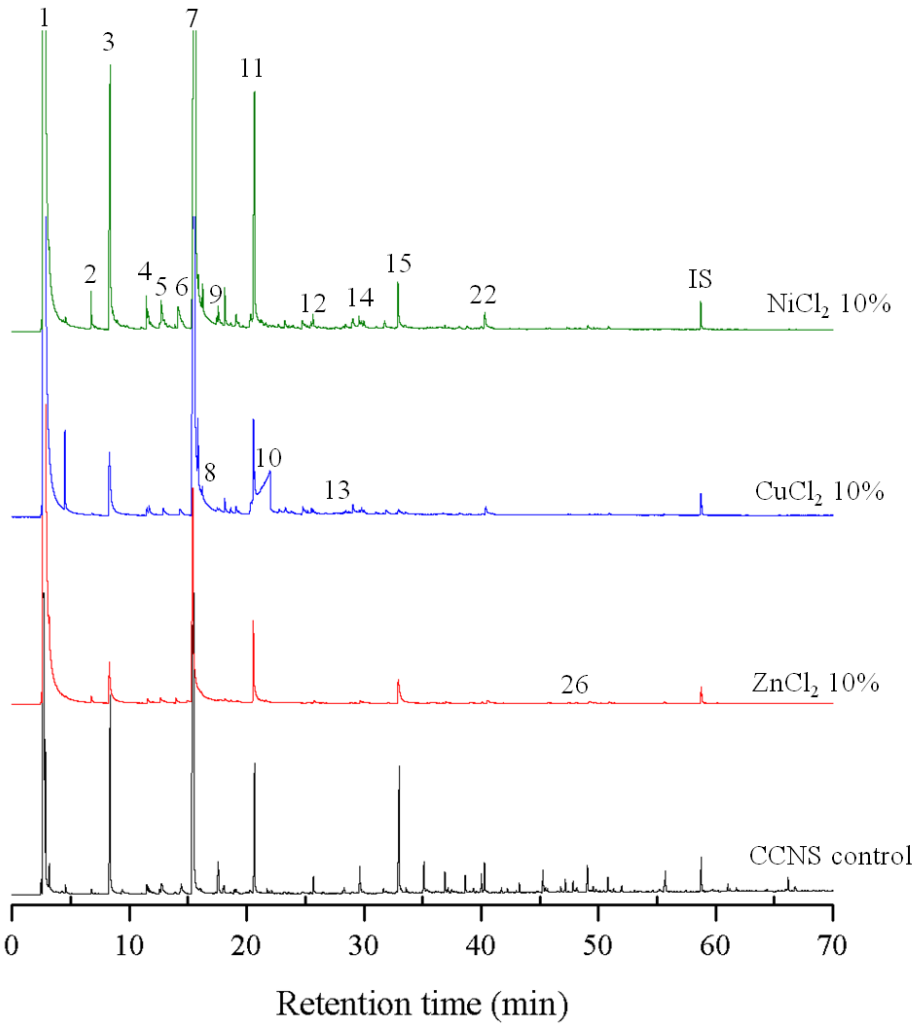

Fig. 13 Gas chromatogram of chemical compounds in HTL oil from CCNS with use of various transition metal chlorides

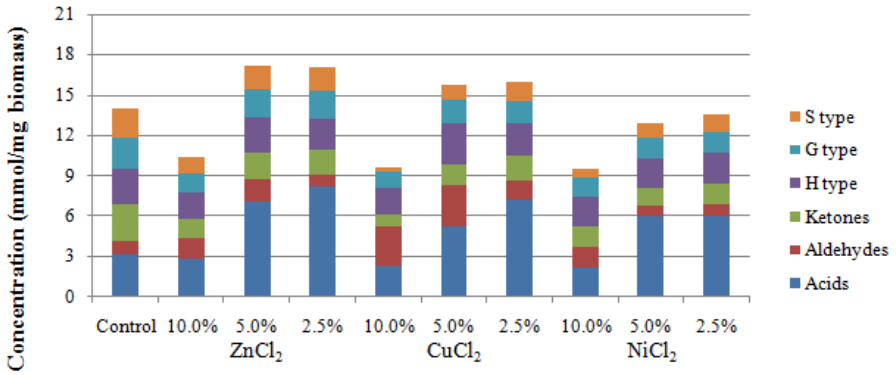

Fig. 14 Amount of different chemical compound groups in HTL oil from EFB with use of various transition metal chlorides

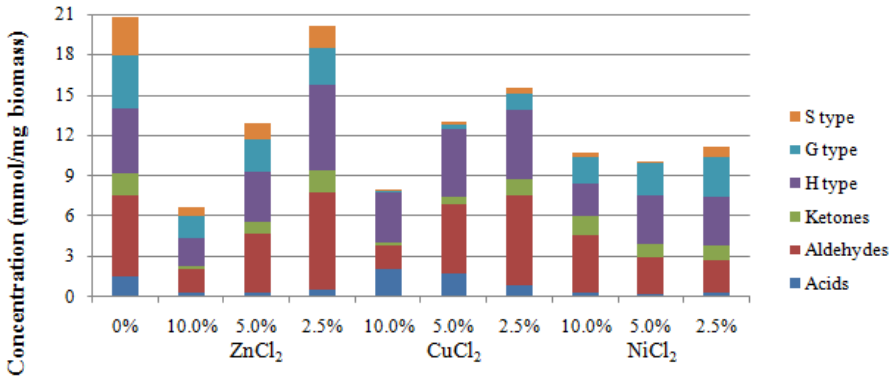

Fig. 15 Amount of different chemical compound groups in HTL oil from CCNS with use of various transition metal chlorides

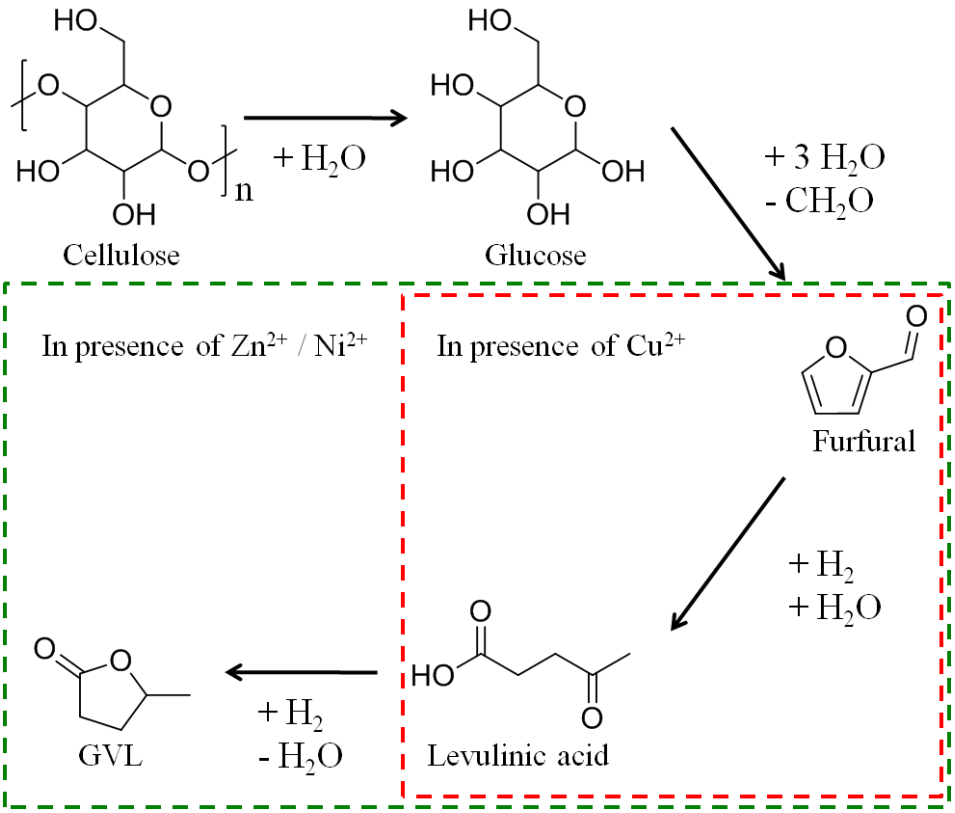

Fig. 16 Proposed pathway of acidic hydrothermal decomposition of cellulose in the presence of transition metal chlorides

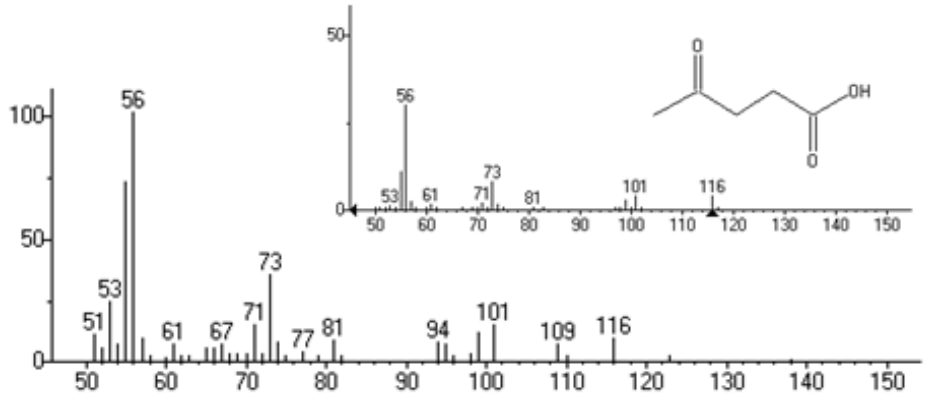

Fig. 17 Mass fragment of levulinic acid compared to the data from NIST mass spectral library

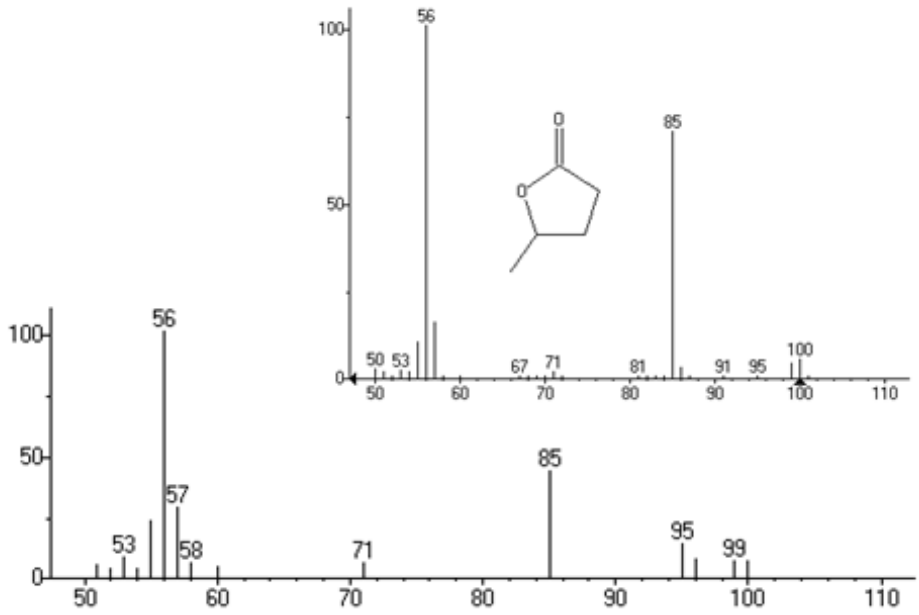

Fig. 18 Mass fragment of GVL compared to the data from NIST mass spectral library

5. Conclusion

The HTL processes of agricultural residues (EFB and CCNS) under different temperature range (240-330 ℃) were performed to investigate the effects of temperature. Then the processes with transition metal chlorides ($ZnCl_2$, $CuCl_2$ and $NiCl_2$) were carried out to determine behaviors of the transition metals during HTL. Mass distribution of HTL products, physicochemical properties of liquid oil and acidity of water phase were affected by reaction temperature. The highest HTL oil yields from EFB and CCNS were all obtained at 300 ℃. Water content decreased down to 300 ℃, and then increased slightly at 330 ℃, while TAN value and the total amount of chemical compounds in HTL oil showed the opposite tendency. Catalytic HTL with transition metal catalysts were performed and the effect on HTL was revealed. Transition metal chlorides became acidic in water, contributed to both depolymerization and repolymerization of liquid products and then converted from liquids to gaseous, WSF or hydrochar. Consequently, transition metals reduced the yield of HTL oil. In the presence of the metals, water content of HTL oil increased, the overall TAN value decreased, and pH of water phase decreased. The chemical composition of HTL oil was characterized by GC/MS analysis. Decrease of compound concentration was found and GVL and levulinic acid were detected. Especially with $CuCl_2$, large amounts of levulinic acid were detected which are known as intermediates from hydrothermal decomposition of cellulose. Proposed pathway suggests that Cu^{2+} ions from $CuCl_2$ disrupt the hydrogenation of levulinic acid and the

conversion from levulinic acid to GVL.

6. References

Abdullah, N., Gerhauser, H. 2008. Bio-oil derived from empty fru it bunches. *Fuel*, **87**(12), 2606-2613.

Ahn, B.-J., Han, G.-S., Choi, D.-H., Cho, S.-T., Lee, S.-M. 2014. Assessment of The Biomass Potential Recovered from Oil Palm Plantation an Crude Palm Oil Production in Indones ia. *Journal of The Korean Wood Science and Technology*, **42**(3), 231-243.

Akhtar, J., Amin, N.A.S. 2011. A review on process conditions fo r optimum bio-oil yield in hydrothermal liquefaction of bio mass. *Renewable and Sustainable Energy Reviews*, **15**(3), 1 615-1624.

Akhtar, J., Kuang, S.K., Amin, N.S. 2010. Liquefaction of empty palm fruit bunch (EPFB) in alkaline hot compressed water. *Renewable Energy*, **35**(6), 1220-1227.

Aysu, T., Durak, H. 2015. Assessment of avocado seeds (Persea a mericana) to produce bio-oil through supercritical liquefacti on. *Biofuels, Bioproducts and Biorefining*, **9**(3), 231-257.

Barbier, J., Charon, N., Dupassieux, N., Loppinet-Serani, A., Mah é, L., Ponthus, J., Courtiade, M., Ducrozet, A., Quoineaud, A.-A., Cansell, F. 2012. Hydrothermal conversion of ligni n compounds. A detailed study of fragmentation and conde nsation reaction pathways. *Biomass and Bioenergy*, **46**, 479 -491.

Boocock, D.G.B., Sherman, K.M. 1985. Further Aspects of Powde

red Poplar Wood Liquefaction by Aqueous Pyrolysis. *The Canadian Journal of Chemical Engineering*, **63**(4), 627-633.

Bridgwater, A.V. 2012. Review of fast pyrolysis of biomass and product upgrading. *Biomass and Bioenergy*, **38**, 68-94.

Brunner, G. 2014. *Hydrothermal and Supercritical Water Processes*. Elsevier.

Christensen, P.R., Mørup, A.J., Mamakhel, A., Glasius, M., Becker, J., Iversen, B.B. 2014. Effects of heterogeneous catalyst in hydrothermal liquefaction of dried distillers grains with solubles. *Fuel*, **123**, 158-166.

Demirbas, A. 2007. Progress and recent trends in biofuels. *Progress in Energy and Combustion Science*, **33**(1), 1-18.

Demirbas, A. 2005. Thermochemical Conversion of Biomass to Liquid Products in the Aqueous Medium. *Energy Sources*, **27**(13), 1235-1243.

Duan, P., Savage, P.E. 2011. Hydrothermal Liquefaction of a Microalga with Heterogeneous Catalysts. *Industrial & Engineering Chemistry Research*, **50**(1), 52-61.

Elliott, D.C., Biller, P., Ross, A.B., Schmidt, A.J., Jones, S.B. 2015. Hydrothermal liquefaction of biomass: developments from batch to continuous process. *Bioresour Technol*, **178**, 147-56.

Eom, I.Y., Kim, J.Y., Kim, T.S., Lee, S.M., Choi, D., Choi, I.G., Choi, J.W. 2012. Effect of essential inorganic metals on primary thermal degradation of lignocellulosic biomass. *Bioresour Technol*, **104**, 687-694.

Eom, I.Y., Kim, K.H., Kim, J.Y., Lee, S.M., Yeo, H.M., Choi, I. G., Choi, J.W. 2011. Characterization of primary thermal d egradation features of lignocellulosic biomass after removal of inorganic metals by diverse solvents. *Bioresour Technol*, **102**(3), 3437-44.

Geng, A. 2013. Conversion of Oil Palm Empty Fruit Bunch to B iofuels. in: *Liquid, Gaseous and Solid Biofuels - Conversio n Techniques*, (Ed.) Z. Fang, InTech, pp. 479-490.

Hakeem, K.R., Jawaid, M., Rashid, U. 2014. *Biomass and Bioene rgy: Applications*. Springer International Publishing.

Harry, I., Ibrahim, H., Thring, R., Idem, R. 2014. Catalytic subcri tical water liquefaction of flax straw for high yield of furf ural. *Biomass and Bioenergy*, **71**, 381-393.

Hwang, H., Oh, S., Cho, T.S., Choi, I.G., Choi, J.W. 2013. Fast pyrolysis of potassium impregnated poplar wood and chara cterization of its influence on the formation as well as pro perties of pyrolytic products. *Bioresour Technol*, **150**, 359-6 6.

Kamio, E., Sato, H., Takahashi, S., Noda, H., Fukuhara, C., Oka mura, T. 2007. Liquefaction kinetics of cellulose treated by hot compressed water under variable temperature condition s. *Journal of Materials Science*, **43**(7), 2179-2188.

Karagöz, S., Bhaskar, T., Muto, A., Sakata, Y., Oshiki, T., Kishim oto, T. 2005. Low-temperature catalytic hydrothermal treat ment of wood biomass: analysis of liquid products. *Chemic al Engineering Journal*, **108**(1-2), 127-137.

Karagoz, S., Bhaskar, T., Muto, A., Sakata, Y. 2006. Hydrotherma l upgrading of biomass: effect of K2CO3 concentration and biomass/water ratio on products distribution. *Bioresour Tec hnol*, **97**(1), 90-8.

Kerdsuwan, S., Laohalidanond, K. 2011. Renewable Energy from Palm Oil Empty Fruit Bunch. in: *Renewable Energy - Tren ds and Applications*, (Ed.) M. Nayeripour, InTech, pp. 124-150.

Kumar, S., Gupta, R.B. 2009. Biocrude Production from Switchgr ass Using Subcritical Water. *Energy & Fuels*, **23**(10), 5151 -5159.

López Barreiro, D., Prins, W., Ronsse, F., Brilman, W. 2013. Hyd rothermal liquefaction (HTL) of microalgae for biofuel pro duction: State of the art review and future prospects. *Biom ass and Bioenergy*, **53**, 113-127.

Liu, A., Park, Y., Huang, Z., Wang, B., Ankumah, R.O., Biswas, P.K. 2006. Product Identification and Distribution from Hy drothermal Conversion of Walnut Shells. *Energy & Fuels*, **20**(2), 446-454.

Lu, Q., Li, W.-Z., Zhu, X.-F. 2009. Overview of fuel properties o f biomass fast pyrolysis oils. *Energy Conversion and Mana gement*, **50**(5), 1376-1383.

Möller, M., Harnisch, F., Schröder, U. 2013. Hydrothermal liquefa ction of cellulose in subcritical water—the role of crystalli nity on the cellulose reactivity. *RSC Advances*, **3**(27), 1103 5.

Mørup, A.J., Christensen, P.R., Aarup, D.F., Dithmer, L., Mamakh el, A., Glasius, M., Iversen, B.B. 2012. Hydrothermal Liqu efaction of Dried Distillers Grains with Solubles: A Reacti on Temperature Study. *Energy & Fuels*, **26**(9), 5944-5953.

Matsui, T.-o., Nishihara, A., Ueda, C., Ohtsuki, M., Ikenaga, N.-o., Suzuki, T. 1997. Liquefaction of microalgae with iron cat alyst. *Fuel*, **76**(11), 1043-1048.

Metzger, P., Largeau, C. 2005. Botryococcus braunii: a rich sourc e for hydrocarbons and related ether lipids. *Appl Microbiol Biotechnol*, **66**(5), 486-96.

Nasernejad, B., Zadeh, T.E., Pour, B.B., Bygi, M.E., Zamani, A. 2005. Camparison for biosorption modeling of heavy metal s (Cr (III), Cu (II), Zn (II)) adsorption from wastewater b y carrot residues. *Process Biochemistry*, **40**(3-4), 1319-1322.

Nyambo, C., Mohanty, A., Misra, M. 2010. Polylactide-based rene wable green composites from agricultural residues and their hybrids. *Biomacromolecules*, **11**(6), 1654-1660.

Oasmaa, A., Elliott, D.C., Korhonen, J. 2010. Acidity of Biomass Fast Pyrolysis Bio-oils. *Energy & Fuels*, **24**(12), 6548-655 4.

Ramiah, M.V. 1970. Thermogravimetric and Differential Thermal Analysis of Cellulose, Hemicellulose, and Lignin. *Journal of Applied Polymer Science*, **14**(5), 1323-1337.

Rodolfi, L., Chini Zittelli, G., Bassi, N., Padovani, G., Biondi, N., Bonini, G., Tredici, M.R. 2009. Microalgae for oil: strain selection, induction of lipid synthesis and outdoor mass c

ultivation in a low-cost photobioreactor. *Biotechnol Bioeng*, **102**(1), 100-12.

Rogalinski, T., Liu, K., Albrecht, T., Brunner, G. 2008. Hydrolysi s kinetics of biopolymers in subcritical water. *The Journal of Supercritical Fluids*, **46**(3), 335-341.

Ross, A.B., Biller, P., Kubacki, M.L., Li, H., Lea-Langton, A., Jo nes, J.M. 2010. Hydrothermal processing of microalgae usi ng alkali and organic acids. *Fuel*, **89**(9), 2234-2243.

Sasaki, M., Adshiri, T., Arai, K. 2003. Production of Cellulose II from Native Cellulose by Near- and Supercritical Water S olubilization. *Journal of Agricultural and Food Chemistry*, **51**(18), 5376-5381.

Sasaki, M., Fang, Z., Fukushima, Y., Adshiri, T., Arai, K. 2000. Dissolution and Hydrolysis of Cellulose in Subcritical and Supercritical Water. *Industrial & Engineering Chemistry Re search*, **39**(8), 2883-2890.

Serrano-Ruiz, J.C., Luque, R., Campelo, J.M., Romero, A.A. 2012. Continuous-Flow Processes in Heterogeneously Catalyzed Transformations of Biomass Derivatives into Fuels and Che micals. *Challenges*, **3**(2), 114-132.

Shao, J., Agblevor, F. 2015. New Rapid Method for the Determin ation of Total Acid Number (Tan) of Bio-Oils. *American J ournal of Biomass and Bioenergy*.

Singh, R., Balagurumurthy, B., Prakash, A., Bhaskar, T. 2015. Cat alytic hydrothermal liquefaction of water hyacinth. *Bioresou r Technol*, **178**, 157-65.

Sluiter, J.B., Ruiz, R.O., Scarlata, C.J., Sluiter, A.D., Templeton, D.W. 2010. Compositional analysis of lignocellulosic feedst ocks. 1. Review and description of methods. *J Agric Food Chem*, **58**(16), 9043-53.

Soroushian, P., Aouadi, F., Chowdhury, H., Nossoni, A., Sarwar, G. 2004. Cement-bonded straw board subjected to accelerat ed processing. *Cement and Concrete Composites*, **26**(7), 79 7-802.

Toor, S.S., Rosendahl, L., Rudolf, A. 2011. Hydrothermal liquefac tion of biomass: A review of subcritical water technologies. *Energy*, **36**(5), 2328-2342.

Vardon, D.R., Sharma, B.K., Scott, J., Yu, G., Wang, Z., Schidem an, L., Zhang, Y., Strathmann, T.J. 2011. Chemical properti es of biocrude oil from the hydrothermal liquefaction of S pirulina algae, swine manure, and digested anaerobic sludg e. *Bioresour Technol*, **102**(17), 8295-303.

Wahyudiono, Kanetake, T., Sasaki, M., Goto, M. 2007. Decompos ition of a Lignin Model Compound under Hydrothermal C onditions. *Chemical Engineering & Technology*, **30**(8), 1113 -1122.

Xu, C., Etcheverry, T. 2008. Hydro-liquefaction of woody biomass in sub- and super-critical ethanol with iron-based catalysts. *Fuel*, **87**(3), 335-345.

Yan, Y., Xu, J., Li, T., Ren, Z. 1999. Liquefaction of sawdust for liquid fuel. *Fuel Processing Technology*, **60**(2), 135-143.

Yin, S., Tan, Z. 2012. Hydrothermal liquefaction of cellulose to b

io-oil under acidic, neutral and alkaline conditions. *Applied Energy*, **92**, 234-239.

Yuan, X.Z., Tong, J.Y., Zeng, G.M., Li, H., Xie, W. 2009. Comparative Studies of Products Obtained at Different Temperatures during Straw Liquefaction by Hot Compressed Water. *Energy & Fuels*, **23**(6), 3262-3267.

Yusoff, S. 2006. Renewable energy from palm oil – innovation on effective utilization of waste. *Journal of Cleaner Production*, **14**(1), 87-93.

Zhang, B., von Keitz, M., Valentas, K. 2009. Thermochemical liquefaction of high-diversity grassland perennials. *Journal of Analytical and Applied Pyrolysis*, **84**(1), 18-24.

Zhou, C.H., Xia, X., Lin, C.X., Tong, D.S., Beltramini, J. 2011. Catalytic conversion of lignocellulosic biomass to fine chemicals and fuels. *Chem Soc Rev*, **40**(11), 5588-617.

Zhu, Z., Toor, S.S., Rosendahl, L., Yu, D., Chen, G. 2015. Influence of alkali catalyst on product yield and properties via hydrothermal liquefaction of barley straw. *Energy*, **80**, 284-292.

초 록

본 연구에서는 농업 부산물인 empty fruit bunch (EFB)와 코코넛 껍질(coconut shell; CCNS)을 시료로 하여 오토클레이브 반응기를 이용한 수열반응(hydrothermal liquefaction; HTL)을 240~330 °C 범위의 온도조건과 세 종류의 전이 금속 염화물(ZnCl2, CuCl2, NiCl2)을 첨가한 조건에서 실시하였다. 이를 통해 수열반응 과정에서 반응온도와 촉매에 따른 수열처리 주요 산물(HTL oil, hydrochar, WSF, 가스)의 수율 및 물리화학적 특성 변화를 구명하였다. EFB로부터 획득한 HTL oil의 수율은 반응온도가 올라감에 따라 증가하여 300 °C에서 가장 높은 수율(24.2%)을 나타냈으며 이는 같은 온도에서 CCNS로부터 얻은 HTL oil의 수율(14.0%)보다 높았다. 이는 시료의 무기성분 중 칼륨이 water-gas shift 반응을 촉매 작용하는데, 그 함량이 EFB와 CCNS가 각각 11,929, 1,412 ppm으로 큰 차이를 보이기 때문으로 사료된다. 반면, 330°C에서는 두 시료 모두 HTL oil의 수율이 소폭 감소하였다. 온도에 따른 가스의 수율은 HTL oil의 수율에 반비례하는 경향을 나타내었다. 240 °C에서 셀룰로오스의 불완전한 분해로 인해 hydrochar의 수율이 50% 이상으로 나타났으며 온도가 상승함에 따라 감소하였다. HTL oil의 수분함량은 EFB와 CCNS가 각각 2.0~5.6%, 3.3~9.6% 범위의 값을 나타내었다. 오일의 전산가(total acid number, TAN)는 EFB와 CCNS가 각각 300 °C, 270 °C에서 가장 높은 값을 보였고 330 °C에서 소폭 감소하였다. 기체크로마토그래프 분석을 통해 EFB로부터 획득한 HTL oil에서는 10종의 홀로셀룰로오스 유래 물질(furfural, cyclic ketones 등)과 18

종의 리그닌 유래 물질(phenol, guaiacol, syringol 등)을 검출하였고, CCNS HTL oil에서는 7종의 홀로셀룰로오스 유래 물질과 17종의 리그닌 유래 물질을 검출하였다. 전이 금속 염화물을 적용한 수열반응에서는 두 시료 모두 투입량이 증가할수록 HTL oil 수율이 감소하는 것을 확인하였으며 그 감소폭은 $CuCl_2$ > $NiCl_2$ > $ZnCl_2$ 순으로 나타났다. 반면, WSF, hydrochar, 가스의 수율 변화는 시료와 촉매의 종류에 따라 다른 경향을 보였다. 같은 전이 금속 조건에서도 시료에 따른 수율 변화의 경향이 다른 이유는 분해 과정에서 화학조성의 차이가 핵심적인 인자로 작용하기 때문으로 판단된다. 전이 금속 투입량이 증가함에 따라 HTL oil의 수분함량이 증가하였고 오일 내 화합물의 양이 감소하였다. GC/MS 분석에 의하면, 전이 금속 염화물 조건에서 수열반응을 통해 얻은 HTL oil에는 11~13종의 리그닌 유래 물질이 검출되어 전이 금속을 적용하기 전보다 그 종류가 줄어든 반면, 홀로셀룰로오스 유래 물질은 10~11종이 검출되어 기존 조건에서의 결과와 같거나 다소 늘어나는 경향을 보였다. 특히 산 용액 조건에서 셀룰로오스의 수열 분해를 통해 생성되는 것으로 알려진 γ-Valerolactone(GVL)과 levulinic acid가 검출되었으며, $CuCl_2$ 조건에서는 다른 조건과 반대로 HTL oil 내 levulinic acid의 양이 GVL에 비해 많은 것으로 나타났다. 이러한 결과로 미루어 ZnCl2, NiCl2는 산 용액 수열 조건에서 셀룰로오스로부터 GVL이 생성되는 분해 과정을 촉진하는 것으로 생각된다. 반면, CuCl2는 앞서 언급한 분해 과정에서 levulinic acid로부터 GVL이 생성되는 수소 첨가 반응을 억제하는 것으로 판단된다.